Geoderma 449 (2024) 116993

Contents lists available at ScienceDirect

Geoderma

journal homepage: www.elsevier.com/locate/geoderma

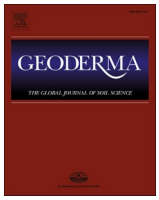

Soil organic matter properties drive microbial enzyme activities and greenhouse gas fluxes along an elevational gradient

Xingguo Han [a,*], Anna Doménech-Pascual [b], Joan Pere Casas-Ruiz [b], Jonathan Donhauser [c], Karen Jordaan [d], Jean-Baptiste Ramond [d,e], Anders Priemé [c,f], Anna M. Romaní [b], Aline Frossard [a]

[a] Forest Soils and Biogeochemistry, Swiss Federal Institute for Forest, Snow and Landscape Research (WSL), Birmensdorf, Switzerland
[b] Research Group on Ecology of Inland Waters (GRECO), Institute of Aquatic Ecology, University of Girona, Girona, Spain
[c] Department of Biology, University of Copenhagen, Copenhagen, Denmark
[d] Centre for Microbial Ecology and Genomics, Department of Biochemistry, Genetics and Microbiology, University of Pretoria, Pretoria, South Africa
[e] Extreme Ecosystem Microbiomics & Ecogenomics (E^2ME) Lab., Facultad de Ciencias Biológicas, Pontificia Universidad Católica de Chile, Santiago, Chile
[f] Center for Volatile Interactions (VOLT), University of Copenhagen, Copenhagen, Denmark

ARTICLE INFO

Handling Editor: C. Rumpel

Keywords:
Greenhouse gas fluxes
Mountainous soils
Elevational gradient
SOM quantity and composition
Microbial enzyme activities and gene functions

ABSTRACT

Mountain ecosystems, contributing substantially to the global carbon (C) and nitrogen (N) biogeochemical cycles, are heavily impacted by global changes. Although soil respiration and microbial activities have been extensively studied at different elevation, little is known on the relationships between environmental drivers, microbial functions, and greenhouse gas fluxes (GHGs; carbon dioxide [CO_2], methane [CH_4] and nitrous oxide [N_2O]) in soils of different elevation. Here, we measured how *in situ* GHG fluxes were linked to soil properties, soil organic matter (SOM) quantity and composition (the proportion of humic-like vs. protein-like OM), microbial biomass, enzyme activities and functional gene abundances in natural soils spanning an elevational gradient of ~2400 m in Switzerland. Soil CO_2 fluxes did not significantly vary from low (lowland zone) to higher (montane and subalpine zones) elevation forests, but decreased significantly ($P<0.001$) from the treeline to the mountain summit. Multivariate analyses revealed that CO_2 fluxes were controlled by C-acquiring enzymatic activities which were mainly controlled by air mean annual temperature (MAT) and SOM quantity and composition. CH_4 fluxes were characterized by uptake of atmospheric CH_4, but no trend was observed along the elevation. N_2O fluxes were also dominated by uptake of atmospheric N_2O. The flux rates remained stable with increasing elevation below the treeline, but decreased significantly ($P<0.001$) from the treeline to the summit. N_2O fluxes were driven by specific nitrifying and denitrifying microbial genes (ammonia-oxidizing *amo*A and N_2O-producing *nor*B), which were again controlled by SOM quantity and composition. Our study indicates the treeline as a demarcation point changing the patterns of CO_2 and N_2O fluxes along the elevation, highlighting the importance of SOM quantity and composition in controlling microbial enzyme activities and GHG fluxes.

1. Introduction

Soils are globally important sources of greenhouse gases (GHGs) from which the most important are carbon dioxide (CO_2), methane (CH_4), and nitrous oxide (N_2O) (IPCC, 2014). Global annual net GHG emissions from soils have been estimated to be over 350 Petagram CO_2-C equivalents (i.e. total effects of CO_2, CH_4, and N_2O normalized to CO_2), which corresponds to about 21 % of the global carbon (C) and nitrogen (N) pools in soils and to more than 10 times the annual CO_2 emissions from fossil fuels (Oertel et al., 2016; Stocker, 2014). Moreover, CO_2 emissions from soil ecosystems have been predicted to increase under climate change (i.e. warming) (Davidson & Janssens, 2006; Melillo et al., 2017; Pries et al., 2017).

Covering approximately 25 % of the Earth's land surface, mountain regions contribute considerably to GHGs emissions and the global C and N cycles (Donhauser & Frey, 2018). Spanning over a wide range of elevation, mountain regions encompass different climatic zones/conditions, with varying soil physico-chemical properties and vegetation

* Corresponding author.
E-mail address: xingguo.han@wsl.ch (X. Han).

https://doi.org/10.1016/j.geoderma.2024.116993
Received 16 January 2024; Received in revised form 2 July 2024; Accepted 2 August 2024
Available online 7 August 2024

Table 1
Sampling sites characteristics. ND: non-detectable. Mean annual temperature: MAT. Mean annual precipitation: MAP. Soil MAT was measured for one year by hygrochron ibutton® [DS1923]) and air MAT and MAP were extracted from the worldclim version 2 (https://worldclim.org/data/worldclim21.html).

Sites	Coordinates	Landcover type	Dominant plant species	Elevation (m a.s.l.)	MAP (mm)	Air MAT [°C]	Soil MAT [°C]	*In situ* T_{soil} [°C]	Sand (%)	Silt (%)	Clay (%)
Vordemwald	N47°16.402′, E007°53.204	Temperate and mixed forests	*Fagus sylvatica* L., *Carpinus betulus* L., *Abies alba* L., *Pinus sylvestris* L., *Larix decidua* Mill.	530	1212.9	9.0	9.9	14.6	50.5	39.9	9.7
Schänis	N47°09.888′, E009°03.982	Temperate broadleaved and deciduous forests	*Fagus sylvatica* L., *Acer platanoides* L.	713	1458.2	8.1	ND	14.7	40.5	31.5	28.1
Sihltalhütte	N47°04.213′, E008°51.613	Temperate broadleaved and deciduous forests	*Fagus sylvatica* L., *Fragaria vesca* L., *Athyrium filix-femina* L.,	971	1589.1	6.6	ND	14.1	10.3	51	38.8
Alpthal	N47°02.874′, E008°42.757	Montane coniferous forests	*Picea abies* L., *Abies alba* L.,	1159	1635.9	6.1	7.6	11.8	55.5	49.9	24.7
Lantsch	N46°41.868′, E009°33.865	Montane coniferous forests	*Picea abies* L., *Abies alba* L., *Pinus sylvestris* L.	1443	1300.3	4.7	ND	13.8	58.2	21.8	20.1
Celerina	N46°29.523′, E009°53.424	Subalpine coniferous forests	*Pinus cembra* L.	1844	798.8	1.3	4.5	10.1	47.1	45.4	7.6
Umbrail Forest	N46°35.010′, E010°26.424	Subalpine coniferous forests	*Pinus sylvestris* L.	2001	535.4	1.3	ND	12.8	72.4	18.7	9.0
Umbrail Treeline	N46°33.967′, E010°26.107	Subalpine coniferous forests	*Pinus cembra* L.with *Dryas octopetala* L.	2114	570.0	0	ND	11.9	6.1	78.2	13.9
Umbrail Meadow	N46°33.219′, E010°26.057	Alpine meadow	*Carex curvula* All.	2336	616.7	– 1.1	4.2	13.6	52.6	26.5	21.0
Umbrail Water	N46°32.580′, E010°25.871	Alpine meadow	*Carex curvula* All., *Anemone alpina* L.,	2543	685.6	– 2.0	ND	10.7	4.0	71.4	18.6
Umbrail Ruins	N46°32.932′, E010°25.450	Alpine meadow	*Anthyllis vulneraria* L., *Saxifraga bryoides* L., *Silene acaulis* L., *Saxifraga exarata Vill.*	2715	739.5	– 2.5	ND	9.9	6.1	78.5	14.2
Umbrail Summit	N46°33.097′, E010°25.108	High Alpine	ND	2959	807.4	– 3.2	– 0.2	9.6	89.7	9.5	0.9

cover (Barry, 2008; Donhauser & Frey, 2018; Kammer et al., 2009) that potentially lead to distinct microbial activities and rates of GHGs fluxes along elevational gradients. Nevertheless, the relationships between environmental drivers, microbial enzyme activities, and GHG fluxes in soils of different elevation remain unclear. Over the last decades, a number of studies have investigated soil respiration and microbial biomass, activities and communities at different elevational scales across the world (reviewed in (Donhauser & Frey, 2018; He et al., 2020; Looby & Martin, 2020)). However, the only studies evaluating soil GHG fluxes over an elevational gradient focused either on managed soils (Fatumah et al., 2019; Hagedorn & Joos, 2014; Imer et al., 2013) or (sub)tropical montane forest soils (He et al., 2016; Ma et al., 2019; Martinson et al., 2013; Martinson et al., 2021; Müller et al., 2016; Neto et al., 2011; Purbopuspito et al., 2006; Teh et al., 2014; Wolf et al., 2012). Temperate montane forests have hardly been studied, and their studies have almost exclusively focused on soil respiration (CO_2) rather than including the three main GHGs (Badraghi et al., 2021; Bardelli et al., 2017; Janssens et al., 2001; Kobler et al., 2019; Rodeghiero & Cescatti, 2005; Shen et al., 2021; Siles et al., 2016). We further note that the only study evaluating concomitantly the three main GHGs in temperate montane forest soils was recently conducted in the Qinling Mountains, China, which showed CO_2 emissions decreased with elevation whereas CH_4 and N_2O fluxes showed no clear relationships with elevation (Pang et al., 2023).

Both climatic and edaphic variables have been recognized as critical factors in controlling soil microbial activities and GHG emissions along elevation gradients. Soil moisture is positively correlated with microbial activity (Orchard & Cook, 1983). Deceasing air and soil temperature with elevation was observed to lower microbial activity, causing the reduction of CO_2 emissions (Neto et al., 2011; Pang et al., 2023). Additionally, soil organic matter (SOM) quantity, composition (i.e. the relative proportion of labile and recalcitrant OM) and accessibility have been shown to be a significant driver of microbial growth and metabolism (Schmidt et al., 2011). Increased levels of SOM content and nutrients in higher elevation forests (1724–2000 m above sea level, m a.s.l.) were observed compared to lower elevation forests (545 – 1200 m a.s.l.), resulting in increased microbial activity and soil respiration in more elevated forests, in spite of the lower temperatures at higher elevation (Siles et al., 2017; Siles et al., 2016). An increased humification degree of SOM due to the increased input of recalcitrant coniferous litter with high C/N ratio and lignin with the elevation was also observed (Siles et al., 2017; Siles et al., 2016; Siles & Margesin, 2016). However, the influence of SOM quantity and composition on soil respiration along a large elevational gradient is poorly known.

Methane production usually increases with soil moisture, as wetter soils potentially provide more anaerobic conditions for methanogens (Dutaur & Verchot, 2007; Smith et al., 2003), while oxidation rates of atmospheric CH_4 decrease at high soil water content due to diffusion limitation (Smith et al., 2000). Methane production can be also boosted with increasing soil temperatures as enhanced soil microbial activity decreases O_2 concentration, causing more anaerobic conditions (Butterbach-Bahl et al., 2013). Additionally, CH_4 production is highly coupled with soil dissolved OM, serving as a C source for methanogens (Lu et al., 2000). Studies have found that mountain soils, including forests and grasslands, are a sink of CH_4. However, no relationships between CH_4 fluxes, soil moisture and SOM along the elevation gradient were observed (Imer et al., 2013; Pang et al., 2023; Wolf et al., 2012).

Nitrous oxide production can be promoted with increasing soil temperatures, as temperature affects enzymatic processes involved in N_2O production. Moreover, temperature-induced increases in soil respiration, leading to a reduction of soil O_2 concentrations and the increases in soil anaerobiosis, which facilitates N_2O production (Butterbach-Bahl et al., 2013). Soil moisture also influences N_2O emissions, with N_2O emissions maximizing in the range of 70 – 80 % water filled pore space (Ludwig et al., 2001). As temperature and moisture are often colinear, it is still hard to disentangle the individual effect on N

emissions (Lai & Denton, 2018). Furthermore, while soil moisture increases N_2O production, dry soils can act as net sinks of N_2O (Goldberg & Gebauer, 2009). While SOM has been found to be positively correlated with N_2O emission with the elevation (Pang et al., 2023), N_2O consumption can also be promoted with the increased abundance of microbial *nosZ* genes (nitrous oxide reductase) by fueling denitrifiers with OM (Lazcano et al., 2021).

Here, we investigated the driving factors of microbial enzyme activities associated with GHG fluxes in 12 natural soils in Switzerland along a ~ 2400 m elevational gradient, ranging from 530 to 2959 m a.s.l., transitioning from mixed temperate forests to montane and subalpine forests, alpine meadow and high alpine (nival) zone. We hypothesized that soil GHG fluxes (i.e. CO_2, CH_4, and N_2O) and microbial enzyme activities along the elevational gradient are mainly driven by SOM quantity and composition (i.e. proportion of humic-like vs. protein-like OM). Both SOM quantity and composition are expected to change along the elevation due to the different litter input from lowland deciduous forests, subalpine coniferous forests, alpine grasses, and barren soils on the mountain summit. To test our hypotheses, we measured *in situ* CO_2, CH_4, and N_2O fluxes as well as soil physico-chemical properties, SOM quantity and composition indices (from fluorescence spectroscopy of extracts), extracellular enzyme activities, microbial biomass, and microbial phylogenetic marker abundances of GHG producing and consuming guilds.

2. Materials and methods

2.1. Sites description and soil collection

Field work took place in August 2021. We measured gas fluxes and sampled soils at 12 sites along an altitudinal gradient in Switzerland, ranging from 530 to 2959 m a.s.l. with intervals of 100 – 200 m elevation difference between sites (Table 1, Supplementary Fig. S1). The air mean annual temperature (MAT) decreased from 9.0 to – 3.2 °C with increasing elevation, and the mean annual precipitation (MAP) ranged from 535.4 to 1635.9 mm (Table 1). The top six highest sites (from 2001 to 2959 m a.s.l.) were located in the Biosfera Val Müstair, a protected area next to the Swiss National Park (https://www.val-muestair.ch). The rest of the sites corresponded to Long-Term Forest Ecosystem Research (LWF) sites, managed by the Swiss Federal Institute for Forest, Snow and Landscape Research (WSL) (https://www.wsl.ch/en/forest/forest-development-and-monitoring/long-term-forest-ecosystem-research-lwf/sites.html), except for the site at 971 m (Sihltalhütte), which was located in a protected forest in the Canton of Schwyz, Switzerland. The gradient included temperate broadleaved and deciduous forests (530 – 971 m), montane coniferous forests (1159 – 1443 m), and subalpine coniferous forests (1844 – 2114 m). The "Umbrail treeline" site (2114 m, Table 1) is located at the edge of tree colonization. Above the treeline, Alpine meadow extended up to the "Umbrail ruins" site (2715 m), and rocky soil covered the "Umbrail summit" site (2959 m).

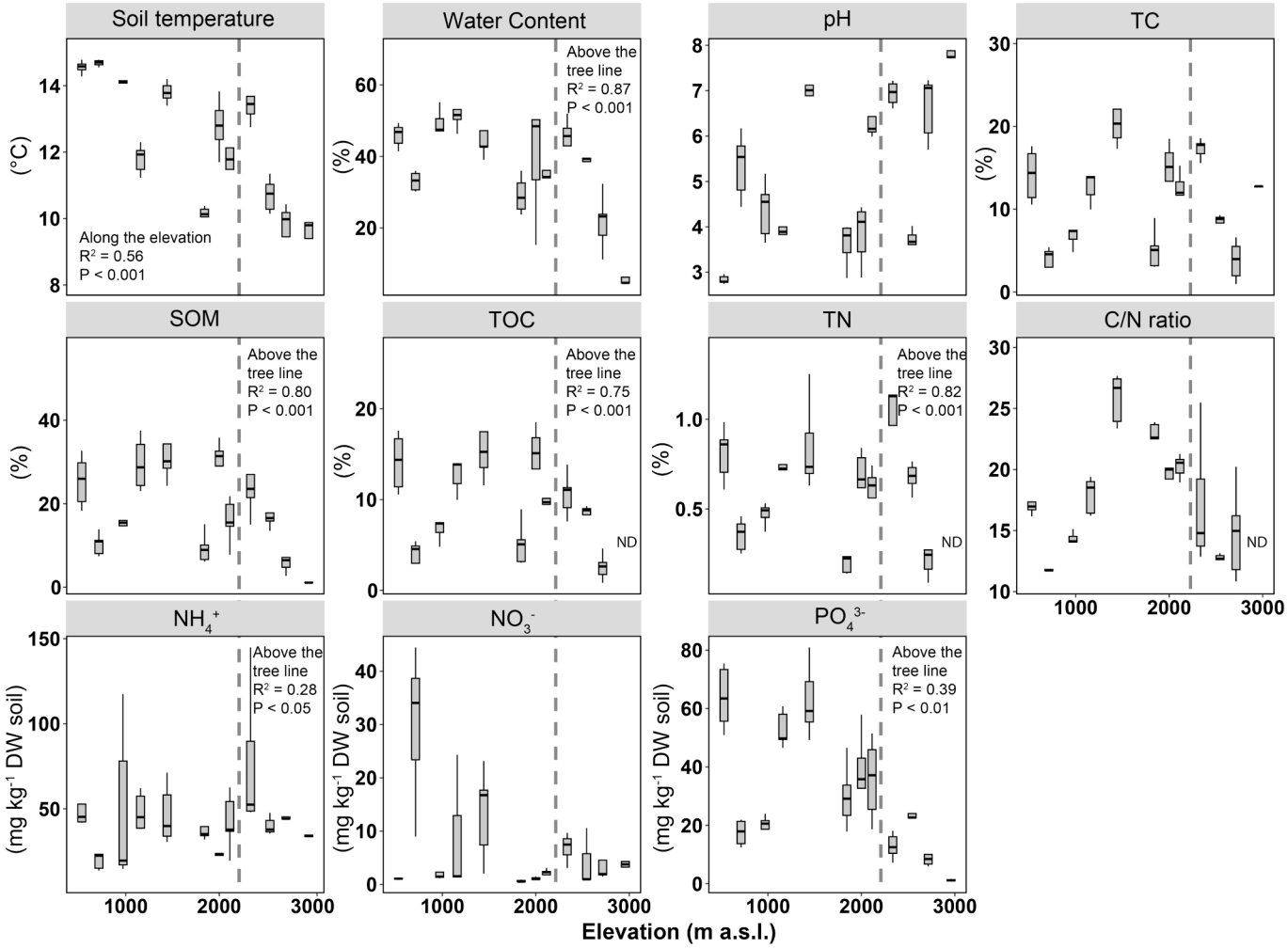

Fig. 1. Soil physico-chemical properties along the elevation gradient at the day of sampling. Sites are ordered from the lowest to highest elevation from left to right. The dashed line indicates the elevation of the treeline. Boxplots were done with 5 replicates for each site (n = 5). ND: non-detectable.

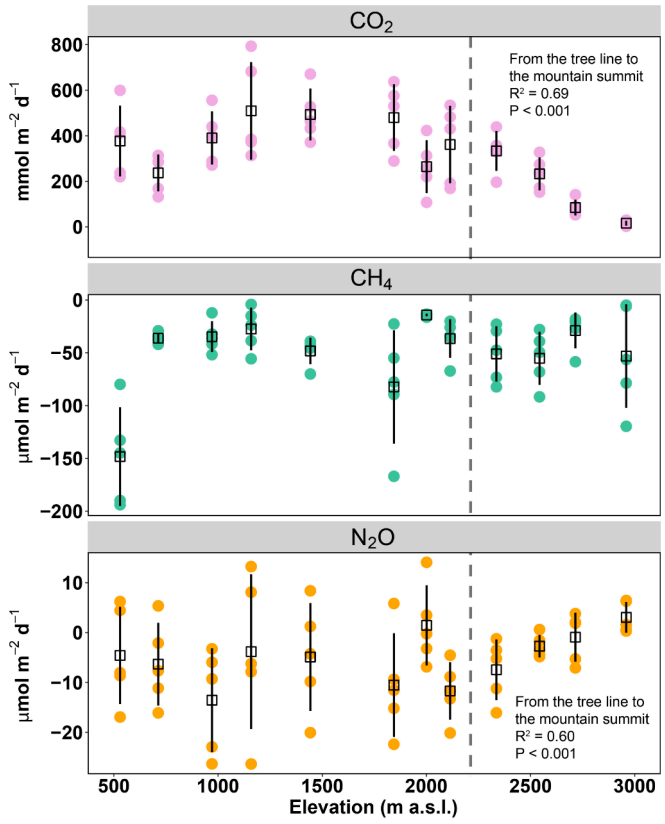

Fig. 2. CO_2, CH_4, and N_2O fluxes along the elevation gradient. Sites are ordered from the lowest to highest elevation from left to right. Squared symbols and vertical lines show the mean and standard deviation of 5 replicates. The dashed line indicates the elevation of the treeline.

At each site, five replicated surface soil samples (top 10 cm using 10-cm diameter PVC tube) were collected randomly within an area of 25 m^2 (total sample number = 60). Soil samples were kept intact in the PVC tube at 4 °C upon collection until being processed (within maximum 72 h). In the lab, samples were 4 mm-sieved, discarding plant and root material as thoroughly as possible. Subsequently, a subsample of the sieved soils was stored at 4 °C for dissolved organic matter (DOM) composition, enzyme assays, and microbial biomass analyses, a second subsample stored at – 20 °C for nutrients and molecular analyses, and a third subsample dried at 60 °C for physico-chemical parameters. Plant litter was collected from each site at five replicated plots within an area of 30 × 30 cm^2. Litter was stored at 4 °C until being dried at 60 °C for 48 h. Subsequently, the mass of the litter was recorded and a subsample was grinded with a Retsch mixer mill (MM 400, Haan, Germany) for C and N content analyses.

2.2. Soil and litter physico-chemical properties

Soil pH was measured in 0.01 M $CaCl_2$ soil solution with a pH meter (2:1 v/w). Soil texture was analyzed using the hydrometer method (Gee & Bauder, 1986). Soil *in situ* gravimetric water content (the percentage of water in the fresh soil: %) was measured by calculating the mass loss by oven-drying fresh soils for 24 h at 105 °C (Gardner et al., 2000). SOM was determined by loss-on-ignition, with a combustion of the samples at 450 °C for 4 h (Davies, 1974). Total carbon (TC) and nitrogen (TN) were measured on dried (60 °C) and fine-grained soils and litter, by an elemental analyzer (NC-2500; CE Instruments, Wigan, United Kingdom). Soil total organic C (TOC) content was quantified after HCl-fumigation using an elemental analyzer (Walthert et al., 2010). Soil ammonium (NH_4^+) and nitrate (NO_3^-) were extracted from 2.5 g dry equivalent soil by 1 M KCl (KCl:soil 4:1 v/w), and filtered through DF 5895–150 ashless paper (Albert LabScience, Dassel, Germany). NH_4^+ in KCl extracts was then determined photometrically with an FIAS 300 flow injection system (Perkin-Elmer, Waltham, MA, USA). NO_3^- in KCl extracts was measured by a DX-120 Ion Chromatograph (Thermo-Scientific, USA). Available phosphorus (phosphate, PO_4^{3-}) was extracted by 0.5 M $NaHCO_3$ ($NaHCO_3$:soil 60:1 v/w), and measured photometrically with Malachite Green using a Tecan plate reader (Life Sciences, USA) (Kuo, 1996).

2.3. GHG fluxes

At each site, five PVC base collars (11 × 10 cm, height × diameter) were inserted into the soils down to a 10 cm depth. Transparent respiration chambers (11 × 10 cm, height × diameter, acrylic glass), connected to an ABB microportable gas analyzer (GLA131-GGA, Quebec, Canada), were tightly placed on the base collars for a continuous measurement of CO_2 and CH_4 fluxes for 5 min (Supplementary Fig. S2). All *in situ* gas fluxes were measured between 09:00 and 11:00 in the morning, for consistency across sites. To perform measurements under dark conditions, respiration chambers were covered by a fully occulting fabric placed at least 10 min prior to the measurements. Gas samples were additionally collected from the respiration chambers with a syringe after 1, 10, 20 and 30 min and stored into pre-vacuumed 12-mL Exetainer vials (Labco, Ceredigion, UK). N_2O content was measured by gas chromatography. Gas concentration was calculated according to the ideal gas law equation $P \times V = n \times R \times T$, where P is pressure (pascals), V is volume (m^3), n is number of molecules (mol), R is the ideal gas constant (8.314 J mol^{-1} K^{-1}), and T is the absolute temperature of the gas (K). GHG fluxes were then calculated by regression of gas concentration against time using the kappa.max method function in the R package gasfluxes (Fuss et al., 2015), as mmol CO_2 m^{-2} d^{-1}, μmol CH_4 m^{-2} d^{-1}, and μmol N_2O m^{-2} d^{-1}.

2.4. SOM composition indices

Water-extractable organic matter (WEOM), including readily available C and nutrients for soil microbes (Zsolnay, 1996), was extracted and

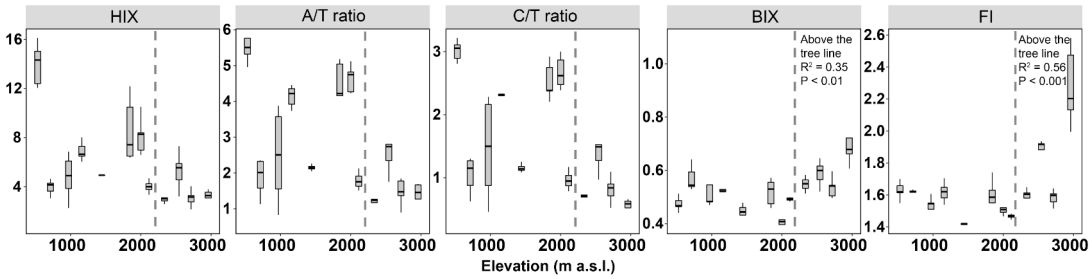

Fig. 3. WEOM composition indices along the elevation gradient. HIX: humification index, BIX: biological index, FI: fluorescence index. Sites are ordered from the lowest to highest elevation from left to right. The dashed line indicates the elevation of the treeline. Boxplots were done with 5 replicates for each site (n = 5).

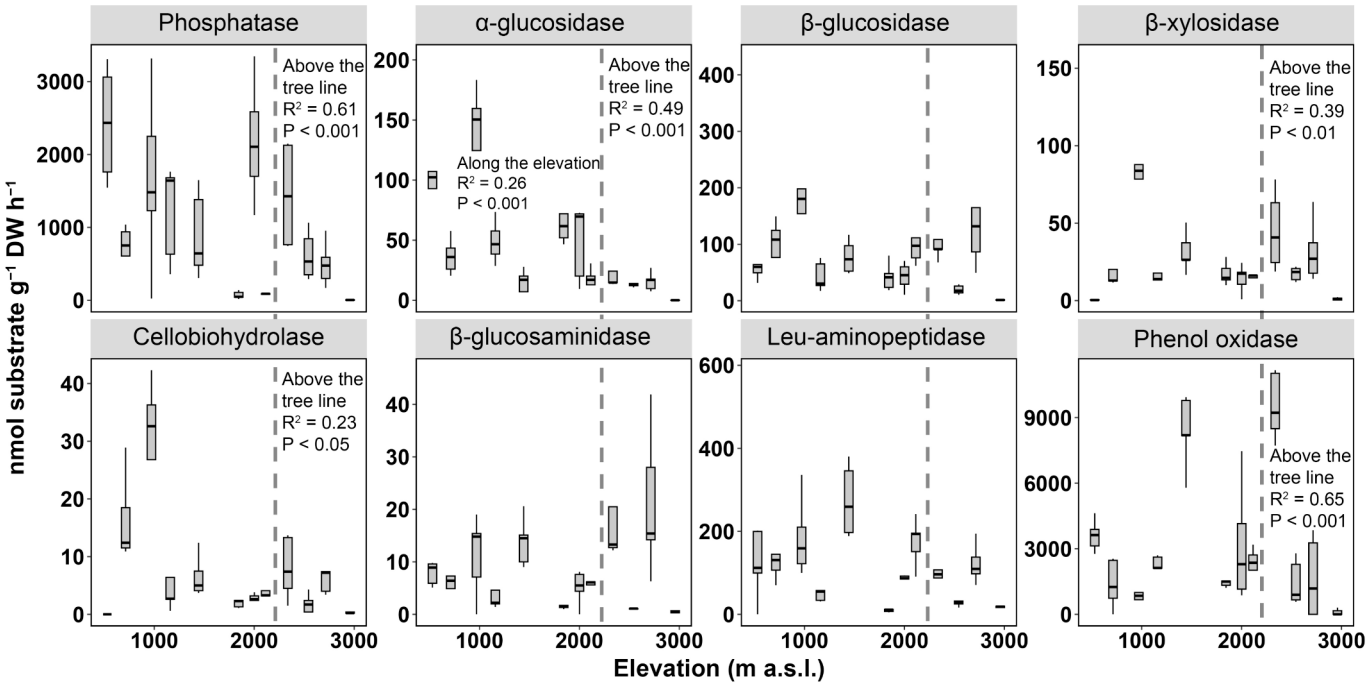

Fig. 4. Soil extracellular enzyme activities along the elevation gradient. Phosphatase (PHOS); α-glucosidase (AG); β-glucosidases (BG); β-xylosidase (BX); Cellobiohydrolase (CEL); β-glucosaminidase (NAG); Leu-aminopeptidase (LAP); Phenol oxidase (POX). Sites are ordered from the lowest to highest elevation from left to right. The dashed line indicates the elevation of the treeline. Boxplots were done with 5 replicates for each site (n = 5).

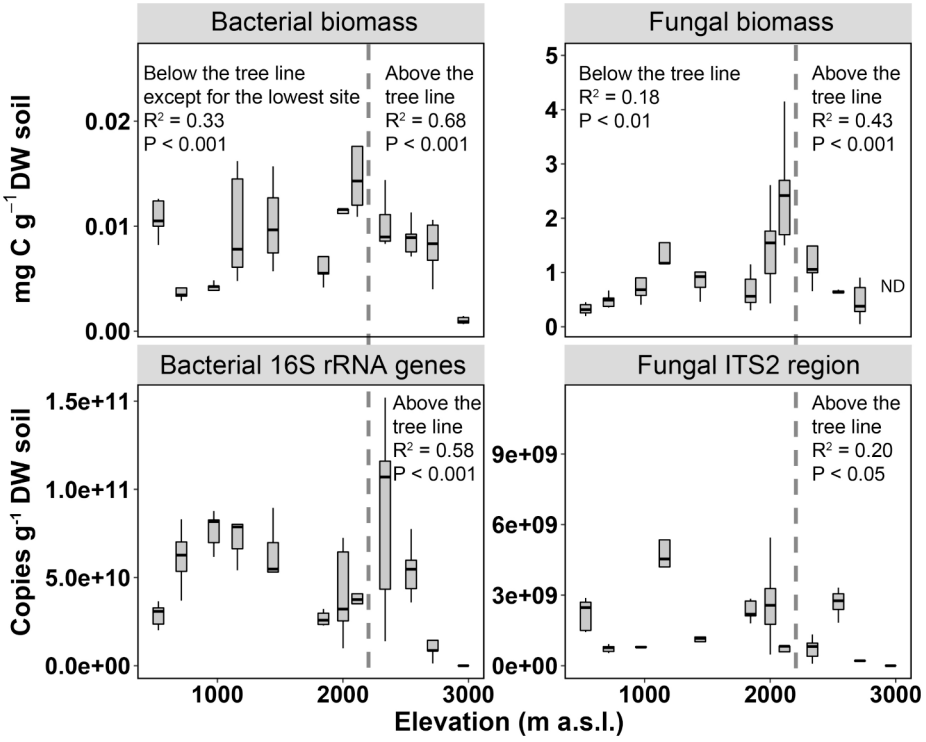

Fig. 5. Bacterial and fungal biomasses, and copies of bacterial 16S rRNA genes and fungal ITS2 region along the elevation gradient. Sites are ordered from the lowest to highest elevation from left to right. The dashed line indicates the elevation of the treeline. Boxplots were done with 5 replicates for each site (n = 5). ND: non-detectable.

measured according to Chantigny et al. (2014). Briefly, 30 g of freeze-dried soil was placed into 250-mL Erlenmeyer flasks with 60 mL of Milli-Q water and incubated with mild agitation (80 rpm) at 20 °C in the dark for 1 h. After incubation, extracts were manually shaken for 5 s, rested for 10–15 min, and filtered through 0.2-μm nylon filters. WEOM composition was characterized by measuring the fluorescence spectra of the extracted dissolved organic matter (DOM) (Fellman et al., 2010). The Fluorescence index (FI) was calculated as the ratio of emission at

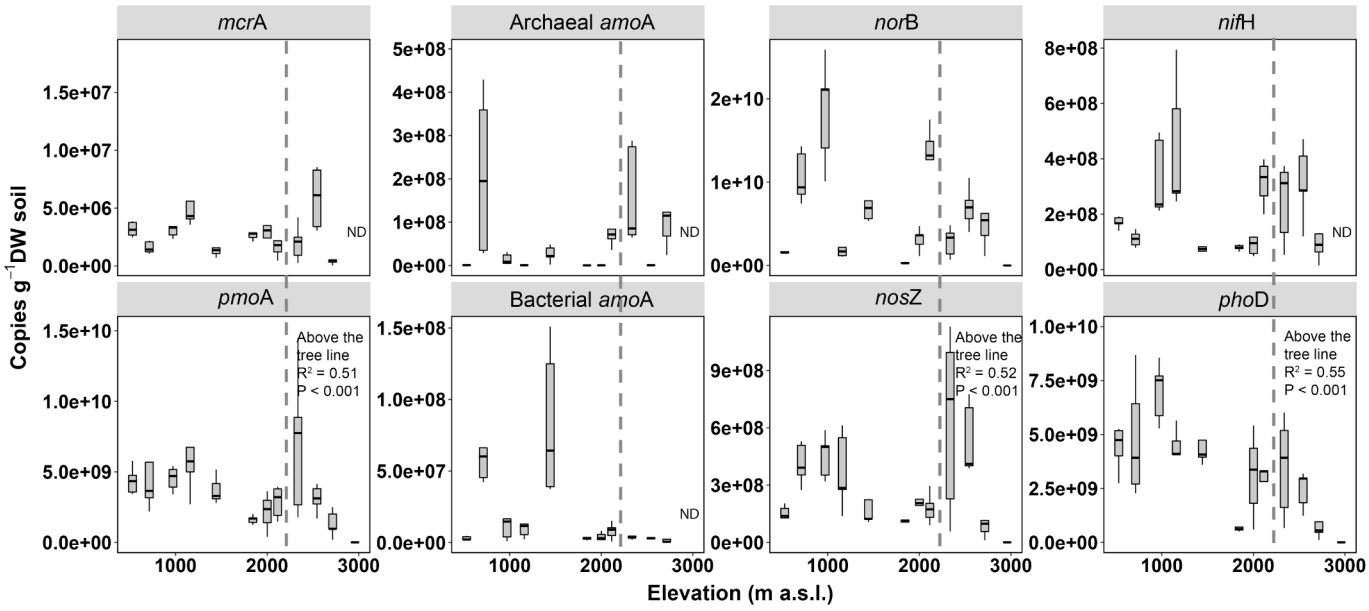

Fig. 6. Copies of methanogenic *mcr*A, methanotrophic *pmo*A, archaeal and bacterial *amo*A, *nor*B, *nos*Z, *nif*H and *pho*D by qPCR along the elevation gradient. Sites are ordered from the lowest to highest elevation from left to right. The dashed line indicates the elevation of the treeline. Boxplots were done with 5 replicates for each site (n = 5). ND: non-detectable.

wavelengths 470 nm and 520 nm at an excitation wavelength of 370 nm, and is an indicator of potential OM source (McKnight et al., 2001). FI values > 1.8 are usually associated with protein-like OM of microbial origin, whereas values close to 1.2 indicate OM with higher humic content derived from vascular plants. The humification index (HIX; unitless) was calculated as the ratio between the peak area under the fluorescence emission spectra 435–480 nm and 300–345 nm at an excitation wavelength of 254 nm (Zsolnay et al., 1999). HIX is related to the aromatic nature and extent of humification of OM, with higher HIX values indicating increased degree of humification (Zsolnay et al., 1999). The biological index (BIX; unitless) was calculated by dividing the fluorescence intensity emitted at 380 nm by that at 430 nm for an excitation of 310 nm (Huguet et al., 2009), with higher BIX values corresponding to the presence of freshly released DOM (Huguet et al., 2009; Wilson & Xenopoulos, 2009). Peak ratio A:T, the ratio of Peak A (ex260/em450) to Peak T (ex275/em304) intensity, and Peak ratio C:T, the ratio of Peak C (ex340/em440) to Peak T (ex275/em304) intensity, are indicators of the relative contribution of humic-like vs. protein-like fluorescence in a sample (Hansen et al., 2016).

2.5. Extracellular enzyme activities

The activity of eight microbial extracellular enzymes, chosen based on their functional involvement in the C, N, and phosphorus (P) cycling, were assessed: (1) β-glucosidase (BG) and (2) cellobiohydrolase (CEL), involved in the degradation of cellulose; (3) α-glucosidase (AG), involved in the degradation of starch; (4) β-xylosidase (BX), involved in the degradation of hemicellulose; (5) N-acetyl-glucosaminidase (NAG), involved in the degradation of chitin and other β-1,4-linked glucosamine polymers; (6) Phosphatase (PHOS), decomposing phosphomonoesters and phosphodiesters; (7) Leucine aminopeptidase (LAP), involved in the degradation of peptides (N-acquiring enzyme); and (8) Phenol oxidase (POX), involved in lignin degradation (polyphenol oxidation and lignin-degrading enzyme). All samples were prepared with an extraction of 5 g of fresh soil with 50 mL of buffer from the same soil pH. Extracts were incubated with the corresponding artificial substrate at saturation conditions in the dark, and at the same temperature as the soil was during the sampling in the field (Supplementary Tables S1 and S2). For hydrolytic enzyme activities (all except Phenol oxidase), at the end of the incubation, glycine buffer (0.05 M, pH 10.4, 1:1, v:v) was added to all samples and standards (0–100 μM for MUF: methylumbelliferyl, and AMC: 7-amino-4-methylcoumarin) as well as to controls for potential sample and artificial substrate fluorescence and quenching. Fluorescence was measured in a microplate reader (TECAN 200 Infinite). Hydrolytic enzyme activities were expressed as the rate of MUF released per hour in relation to dry weight (DW) soil (nmol MUF g^{-1} DW h^{-1}). Phenol oxidase activity was determined by spectrophotometry using L-DOPA (L-3,4-dihydroxyphenylamine) as a model substrate (Pind et al., 1994). Soil extracts with DOPA and controls (extracts without DOPA) were incubated and absorbance measured at the end of incubation (Shimadzu UV-1800). It was expressed in the unit of μmol 2,3-dihydroindole-5,6-quinone-2-carboxylate (DIQC) per g of DW soil per hour (μmol DIQC/g DW h^{-1}).

2.6. Microbial biomass

Bacterial biomass (BB) was extracted from 5 g fresh soil with a detaching solution incubation (30 min, dark conditions, 150 rpm) and purified using the Nycodenz density gradient centrifugation (Nycodenz, OptiPrep, Sigma-Aldrich, Merck KGaA; centrifugation: 90 min, 14000 rpm, 4 °C) (Amalfitano & Fazi, 2008). The supernatant was stained using as nucleic acid stain SYTO13 (FISHER, 5 μM), and a beads solution (106 beads mL^{-1}, FISHER, 1 μm) was added in a known concentration. Stained cells were counted through flow cytometry (FACSCalibur, Becton Dickinson) and expressed per gram of DW soil (cells g^{-1}). BB results were finally expressed as bacterial C per gram of DW (mg bacterial C/g DW soil) through the corresponding conversion factors (Bratbak & Dundas, 1984; Theil-Nielsen & Sondergaard, 1998).

Fungal biomass (FB) was determined by the ergosterol method according to Gessner (2005). For the lipid extraction, samples were lyophilized, incubated with KOH 0.14 M in methanol and added to a hot bath (80 °C, 30 min). After the extraction, samples filtered (GF/F filters, 1.2-μm pore size, Whatman International Ltd.), and charged to solid-phase extraction cartridges for lipid separation (Sep-Pak, V ac RC, tC 18, 500 mg, Waters). Ergosterol was eluted from the cartridges with isopropanol and quantified by high-performance liquid chromatography (Waters Corporation Inc., Milford, MA, USA) at 282 nm. Quantification was based on the comparison with ergosterol standards (0–200 μg/ml,

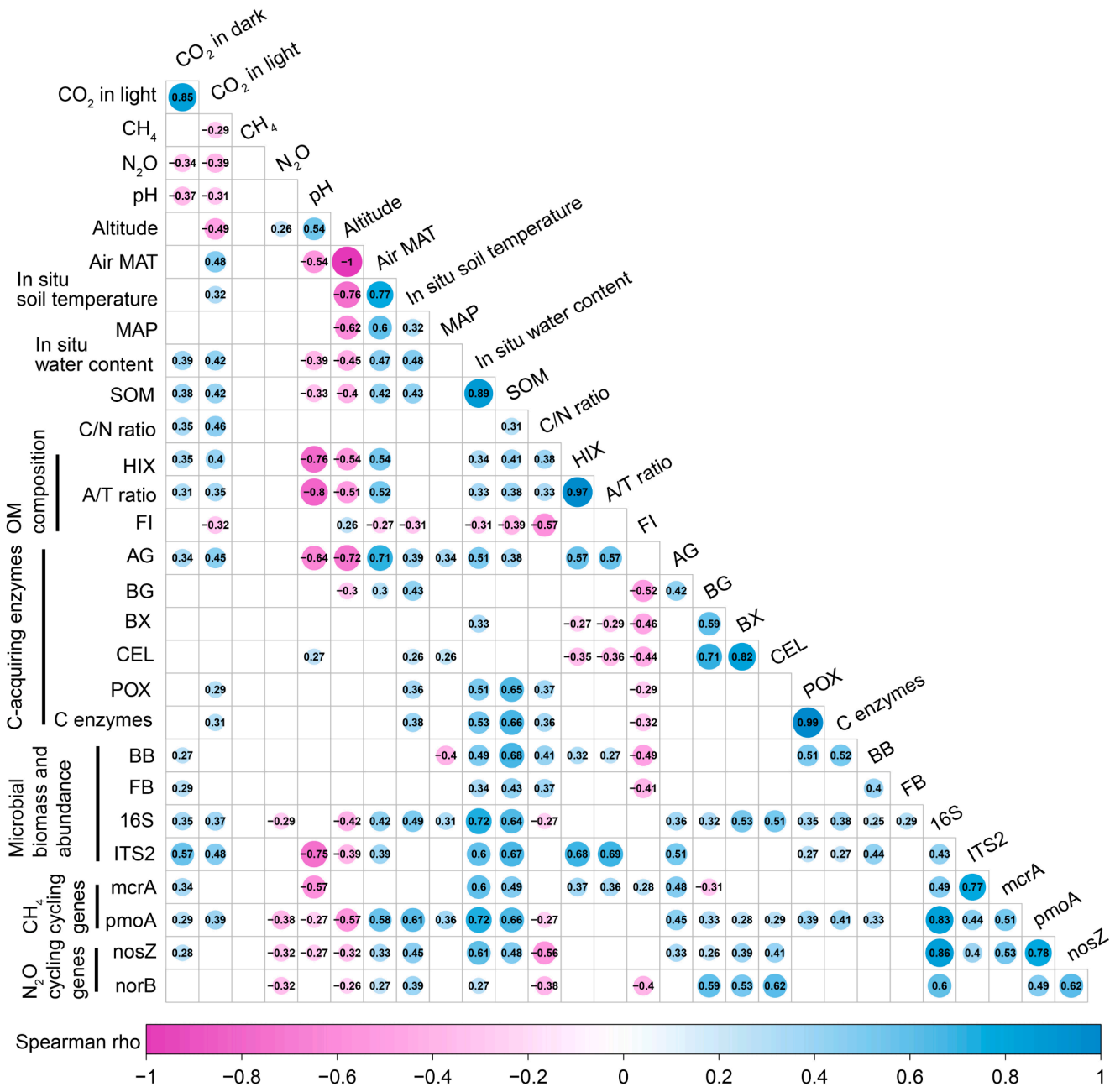

Fig. 7. Heatmap of the significant correlation (P<0.05) relationships among GHG fluxes, environmental and microbial variables along the elevation based on Spearman correlation. Blue and pink represent positive and negative correlations, respectively. The size of the circle indicates the coefficient values, corresponding to the number in the circle. HIX: Humification index; FI: fluorescence index; AG: α-glucosidase; BG: β-glucosidases; BX: β-xylosidase; CEL: Cellobiohydrolase; POX: Phenol oxidase; C enzymes = AG+BG+BX+CEL+POX; BB: Bacterial biomass; FB: Fungal biomass; 16S: 16S rRNA gene; ITS2: Fungal ITS2 region. Data were from 12 sites with 5 replicates for each site (n = 60). (For interpretation of the references to colour in this figure legend, the reader is referred to the web version of this article.)

Fluka Chemical Co., Steinheim, Germany). Results for FB were expressed as fungal C per gram of DW (mg fungal C/g DW soil) through the stoichiometric relationships described by Gessner and Chauvet (1993).

2.7. DNA extraction and quantification of microbial genes

Total DNA was extracted from ~ 0.25 g soil with the DNeasy Powersoil Pro Kit (Qiagen, Hilden, Germany) according to the manufacturer's instructions. DNA was quantified by PicoGreen following the protocol (ThermoFisher Scientific, USA).

The abundance of bacterial 16S rRNA genes, fungal ITS2 region, *mcr*A (Methyl Coenzyme M Reductase A), *pmo*A (particulate methane monooxygenase), *nif*H (nitrogenase reductase), bacterial and archaeal *amo*A (ammonia monooxygenase), *nor*B (nitric oxide reductase), *nos*Z (nitrous oxide reductase), and *pho*D (alkaline phosphatase D) were quantified by qPCR. Microbial gene abundances were determined on a QuantStudio5 Real-Time PCR System (Thermo Fisher Scientific, Waltham, MA, USA) by SYBR-Green based on qPCR according to Han et al. (2023). Each qPCR reaction (10 μL) was composed of 5 μL GoTaq® qPCR Master Mix (Promega), 0.1 μL 30 mg mL^{-1} bovine serum albumin (BSA), 0.5 μL 10 μM of each primer, 1.9 μL molecular-grade water, and 2 μL DNA template. DNA extracts were diluted to a concentration of 2 ng μL^{-1} to avoid PCR inhibition. Details of thermal cycling conditions are described in Supplementary Table S3. Synthetic DNA fragments were

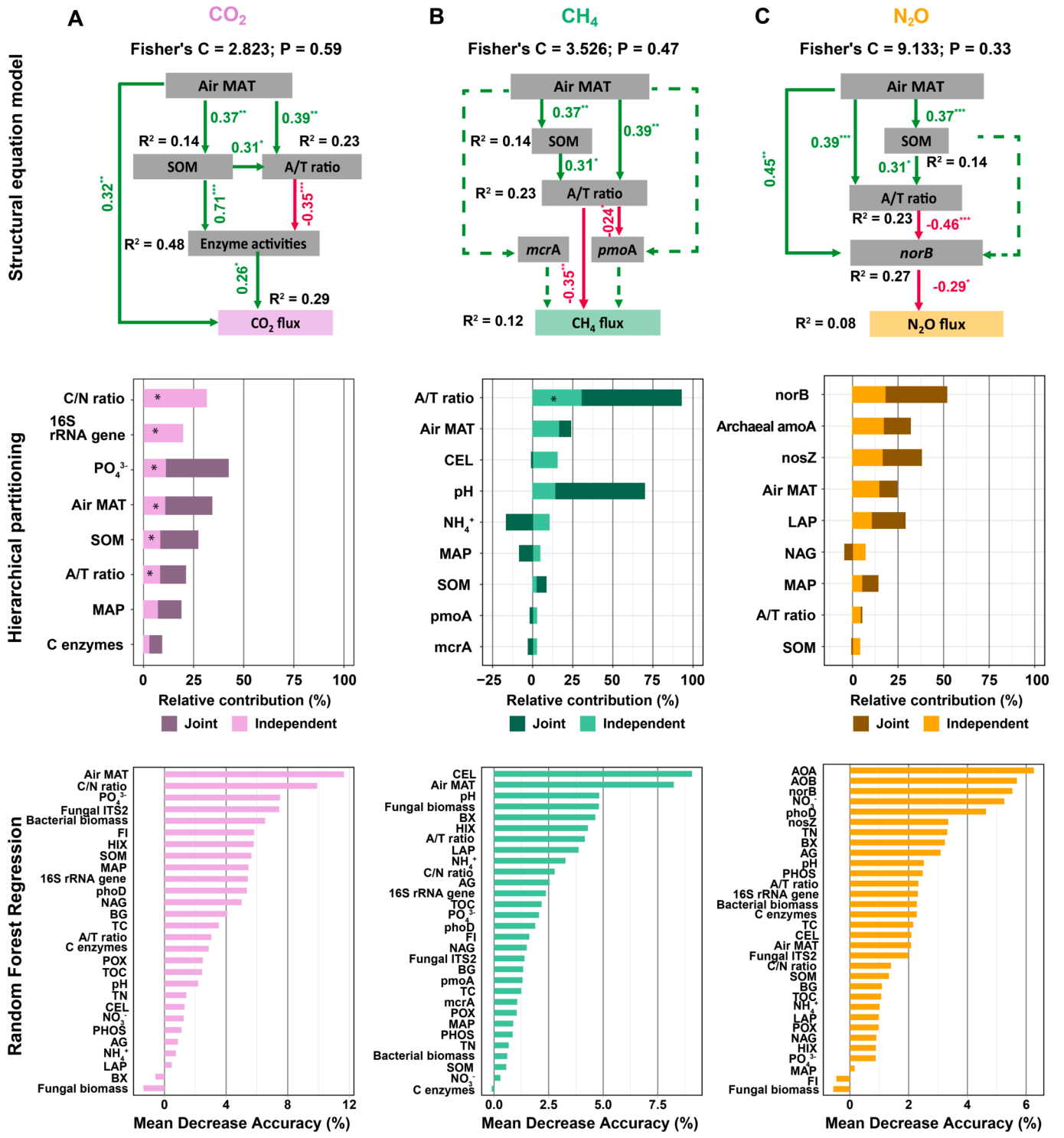

Fig. 8. Structural equation model, Hierarchical partitioning and Random Forest Regression showing the impacts of soil characteristics and microbial activities on GHG fluxes (Column A: CO_2; B: CH_4; C: N_2O) along the elevation gradient. In Structural equation model (top row), the numbers next to the arrows indicate the strength of standardized path coefficients (***P<0.001; **P<0.01; *P<0.05). Only significant impacts are shown. Green arrows represent positive effects and red arrows negative effects. The fraction of explained variation (R^2) for each endogenous variable is highlighted below the variable. The higher A/T ratio (OM composition), the more humic-like SOM is. In Hierarchical partitioning (middle row), * = P<0.05 for significant independent effect. In Random Forest Regression (bottom row), % = Variable importance. Variables with individual importance over 4.0 % and cumulative importance over 70.0 % were considered as the most influential factors. SOM was applied as soil OM quantity, A/T ratio as OM composition and C-acquiring enzymes (AG+BG+BX+CEL+POX) for enzyme activities. Humification index (HIX); biological index (BIX); fluorescence index (FI); α-glucosidase (AG); β-glucosidases (BG); β-xylosidase (BX); Cellobiohydrolase (CEL); β-glucosaminidase (NAG); Leu-aminopeptidase (LAP); Phosphatase (PHOS); Phenol oxidase (POX). C enzymes = AG+BG+BX+CEL+POX. Data were from 12 sites with 5 replicates for each site (n = 60). (For interpretation of the references to colour in this figure legend, the reader is referred to the web version of this article.)

used as qPCR standards according to Han et al. (2023).

2.8. Data analyses

All statistical analyses and plot production were conducted in R v3.4.0 (http://R-project.org) using R Studio v1.1.442 (http://rstudio.com). Relationships between gas fluxes and elevation were done by the best fit (best coefficient of determination: R^2) polynomial regression: y ~ poly(x, 3) with degree n = 3, where x is the elevation and y the gas fluxes. Significant differences between regressions of GHG fluxes, soil and litter properties, OM composition, extracellular enzymes, microbial biomass and gene abundance, along the elevation were tested by linear regression and ANOVAs. Normal distribution was tested by the function shapiro.test() from stats package (https://cran.r-project.org/web/packages/STAT/index.html), visualized by Q-Q plots with the function ggqqplot() from ggpubr package (https://cran.r-project.org/web/packages/ggpubr/index.html). Heteroscedasticity was tested with Breusch Pagan Test by the function ols_test_breusch_pagan() from olsrr package (https://cran.r-project.org/web/packages/olsrr/index.html). A correlation matrix based on Spearman correlation coefficients, including GHG fluxes, environmental variables, enzyme activities, microbial biomass and gene abundances was produced with the functions rcorr() and corrplot() from Hmisc (Harrell and Harrell, 2019) and Corrplot (Wei et al., 2013) packages.

Structural equation modeling (SEM) was applied to the correlated variables to model the effects of environmental drivers on microbial activities and GHG fluxes. Function piecewiseSEM() from piecewiseSEM package was used to calculate the best fit model, following the workflow from https://github.com/jslefche/piecewiseSEM/blob/master/vignettes/piecewiseSEM.Rmd (Lefcheck, 2016). The environmental parameters chosen for SEM analysis (sample number, n = 60) were: air MAT, MAP, SOM quantity, A/T ratio (as OM composition) and microbial enzyme activities (C-acquiring enzymes: AG+BG+BX+CEL+POX for CO_2 model (Zhang et al., 2023)), functional genes abundances of *mcr*A and *pmo*A for CH_4 model, and functional gene abundance of *nor*B and *nos*Z for N_2O model). All variables were scaled according to the formula [(value – mean value)/standard deviation] by the function scale() from base package (https://github.com/SurajGupta/r-source/blob/master/src/library/base/R/scale.R) before being used for the model. According to Spearman correlation, air MAT (coefficient rho = 0.48) was more significantly correlated with CO_2 fluxes than MAP (none significant P>0.05). Since air MAT and MAP were significantly correlated, only air MAT was included in the SEM model to avoid collinearity problems. The best fitting and selected models were the ones that do not reject the null hypothesis (P>0.05), with the highest P value.

We further applied hierarchical partitioning (HP) to address the multicollinearity of variables (Mac Nally, 1996) and to identify the predictors of GHG fluxes by the function hier.part() from the hier.part package (https://github.com/cran/hier.part/blob/master/R/hier.part.R). HP considered all possible response variables in a hierarchical regression setting. Each independent variable had two contributing fractions: independent contribution and joint contribution (relative contribution to shared variability). Negative joint effects were possible for variables that act as suppressors of other variables (Mac Nally & Walsh, 2004). Significance of variables included in HP was calculated using 0.95 confidence of z values (z = 1.65) obtained for each variable with 999 repeated model fits by the function rand.hp() (Mac Nally, 2002). Since HP gave a rounding error when more than 9 predictors were fitted into the model, we kept the predictors number within 9 for each gas model based on Spearman correlations and SEM analysis.

Random forest (RF) regressions (Breiman, 2001) were also implemented to assess the importance of randomly selected variables influencing GHG fluxes with the function randomForest() from randomForest package (https://cran.r-project.org/web/packages/randomForest/index.html). Each model (one model per GHG) included soil physico-chemical parameters (air MAT, MAP, pH, TC, TN, TOC, SOM, C/N ratio, NH_4^+, NO_3^- and PO_4^{3-}), OM composition indices (HIX, A/T ratio and FI), bacterial and fungal biomass and abundance, *pho*D abundance, activities of C-acquiring enzymes (AG, BG, BX, CEL and POX), N-acquiring enzymes (NAG and LAP), and P-acquiring enzyme PHOS. Gene abundances of *mcr*A and *pmo*A involved in CH_4 metabolism were included in the model for CH_4 fluxes. Gene abundances of archaeal and bacterial *amo*A, *nor*B and *nos*Z involved in N cycling were included in the model for N_2O fluxes.

3. Results

3.1. Soil physico-chemical properties

Soil properties showed remarkable variations along the elevational gradient (Fig. 1). Soil pH was lowest and highly acidic (2.8 ± 0.1) at the lowest point of the altitudinal gradient and the highest and slightly alkaline (7.8 ± 0.1) at the most elevated point. However, no clear trend could be observed below or above the tree line. A significant decrease in *in situ* soil temperature was observed with elevation across all sites (P<0.001). Soil *in situ* water content, SOM, TOC, TN, NH_4^+, and PO_4^{3-} decreased significantly (P<0.05) from the treeline (2114 m) to the mountain summit (2959 m). TC also decreased with elevation from the treeline, with the exception of the mountain summit site, which was dominated by inorganic C from calcareous rocks. However, below the treeline, these variables remained relatively stable, and even slightly increased from the low altitudinal temperate forest sites to the subalpine forests for TC, SOM, TOC, TN, C/N ratio and PO_4^{3-}. The Celerina forested site at 1844 m was an outlier in many parameters, such as soil MAT, *in situ* soil temperature, TOC and SOM. This site was located in a valley, therefore receiving less sunlight than sites at higher elevations. In Celerina, the soil MAT and *in situ* soil temperature were similar or lower than those at higher elevations and TOC, SOM and plant litter biomass were lower compared to the neighboring sites (Fig. 1, Supplementary Fig. S7). TN, TOC and C/N ratio were not detectable in the mountain summit samples due to the lack of plant litter input and a majority of calcareous rocks at this site.

3.2. GHG fluxes

CO_2 fluxes showed a humped-shape pattern with increasing elevation (R^2 = 0.35, P<0.001; Fig. 2), where fluxes were the highest at 1159 m (Alpthal, 509.4 ± 240.0 mmol CO_2 m^{-2} d^{-1}) and decreased linearly from the treeline site at 2114 m (361.6 ± 169.7 mmol CO_2 m^{-2} d^{-1}) to the mountain summit at 2959 m (16.3 ± 10.6 mmol CO_2 m^{-2} d^{-1}; R^2 = 0.69, P<0.001). However, no significant variation of CO_2 fluxes was observed when only considering the sites below the treeline, except for a slight increase from the low altitudinal temperate to the subalpine forests. The forest sites showed similar CO_2 fluxes when measured in dark or daylight conditions. However, CO_2 fluxes were lower when measured in daylight condition at the Alpine meadow site (at 2543 m), where the soil surface was covered by a relatively thick layer of grass (Supplementary Fig. S3).

CH_4 fluxes were consistently negative along the elevation gradient, indicating CH_4 oxidation outweighed production at all sites. Measured values of CH_4 fluxes varied between −148.3 ± 46.7 (Vordemwald, 530 m) and −14.2 ± 1.2 (Umbrail forest, 2001 m) μmol CH_4 m^{-2} d^{-1}, but no clear pattern of CH_4 fluxes emerged across the sites along the increasing elevation gradient (Fig. 2).

Below the treeline, N_2O fluxes varied between −13.5 ± 10.4 (Sihltalhütte, 971 m) and 1.5 ± 8.0 (Umbrail forest, 2001 m) μmol N_2O m^{-2} d^{-1}, but no significant variation was observed with elevation (Fig. 2). However, in contrast to CO_2 fluxes, N_2O fluxes increased significantly and linearly (P<0.001) from the treeline site (−11.7 ± 5.8 μmol N_2O m^{-2} d^{-1}) to the summit (3.1 ± 3.1 μmol N_2O m^{-2} d^{-1}). Additionally, below the treeline there was larger within sample site variation, while above the treeline there was much less at each site.

3.3. SOM composition indices

Values of HIX (humification index), A/T and C/T (fluorescence peak ratio A:T and C:T) increased from the low altitudinal temperate forest sites to the treeline (2114 m) (Fig. 3), indicating an increase in the contribution of humic-like OM compared with protein-like OM (Hansen et al., 2016). Above the treeline, these indices drastically decreased with increasing elevation to the mountain summit (2959 m). Contrastingly, the BIX index (biological index), an indicator for autochthonous microbial-derived OM, remained low (<1) across the whole elevation gradient, but increased consistently, significantly, and linearly from the treeline to the summit ($P<0.01$), suggesting a predominantly microbial OM origin above the treeline. The FI index (fluorescence index), indicating the relative contribution of plant-derived and microbial sources to the OM pool, showed the same pattern as the BIX index, increasing significantly and linearly from the treeline to the summit ($P<0.001$) confirming an increasing importance of OM of microbial origin in high altitudinal soils, while OM of terrestrial plant origin contributed more to the OM pool below the treeline.

3.4. Extracellular enzyme activities

Phosphatase (PHOS, P-acquiring enzyme) activity was the highest among all hydrolytic enzyme activities measured, ranging from 5.0 ± 5.1 to 2421.7 ± 774.7 nmol MUF g^{-1} DW h^{-1}, followed by Leucin-aminopeptidase (LAP, N-acquiring enzyme, from to 16.3 ± 17.3 to 274.2 ± 86.4 nmol MUF g^{-1} DW h^{-1}) (Fig. 4). PHOS, and C-acquiring enzymes of β-xylosidase (BX), cellobiohydrolase (CEL) and phenol oxidase (POX), decreased significantly and linearly from the site above the treeline (2336 m) to the summit (2959 m, $P<0.05$). Below the treeline (2114 m), although there were no significant changes of PHOS, BX, CEL and POX in relation to elevation, these enzymes varied considerably across the sites. In addition, POX increased slightly from the low altitudinal temperate forest sites to the subalpine forests. α-glucosidase (AG, C-acquiring enzyme) displayed a significantly and linearly constant decrease with increasing elevation ($P<0.001$).

3.5. Microbial biomass and abundances

Bacterial biomass increased significantly from the low altitudinal temperate forest site at 713 m (i.e., after excluding the lowest site at 530 m) to the treeline site at 2114 m (linear regression for all tests in this section, $P<0.001$, Fig. 5). It then decreased significantly ($P<0.001$) from the treeline site to the mountain summit at 2959 m. Similar to bacterial biomass, abundance of bacterial 16S rRNA gene copies decreased significantly from the site above the treeline at 2336 m to the summit at 2959 m ($P<0.001$).

Fungal biomass increased significantly from the lowest site to the treeline site ($P<0.001$), and then decreased significantly to the summit ($P<0.001$, Fig. 5). Similarly, copies of the fungal ITS2 region decreased significantly from the alpine meadow at 2336 m to the summit ($P<0.05$).

3.6. Functional genes abundance

None of the functional genes measured showed a significant increase or decrease in abundance along the elevation gradient (Fig. 6). However, when considering only the sites above the treeline (i.e., above 2336 m), the abundances of *pmo*A (CH_4 oxidation), *nos*Z (N_2O reduction), and *pho*D (organic P mineralization) decreased significantly with increasing elevation (all $P<0.001$).

3.7. Relationships among GHG fluxes, climatic and edaphic variables, and microbial enzyme activities

To investigate the importance of environmental variables in controlling GHG fluxes and microbial activities along the elevation gradient, correlations among GHG fluxes, climatic and edaphic variables, bacterial and fungal microbial biomasses, microbial functional gene abundances, and potential enzyme activities were compiled in a correlation heatmap (Fig. 7, Supplementary Fig. S4). CO_2 fluxes, under both dark and daylight conditions, were significantly and positively correlated to *in situ* water content, SOM, C/N ratio, OM composition indices HIX and A/T ratio, AG activity, and bacterial and fungal abundances, and negatively correlated only to pH ($P<0.05$). CO_2 fluxes were further positively correlated to bacterial and fungal biomass under dark conditions, and correlated to air MAT, *in situ* soil temperature, POX and C-acquiring enzyme activities under daylight conditions ($P<0.05$). N_2O fluxes were significantly and negatively correlated to the 16S rRNA, archaeal *amo*A, *nor*B and *nos*Z gene abundances along the elevation gradient ($P<0.05$). Although measured only to a depth of 10 cm, significant relationships between GHG and edaphic properties were found despite of being potentially limited by the shallow measurement.

When considering only the sites above the treeline (i.e., from 2336 m and above), N_2O fluxes were negatively correlated to air MAT, *in situ* soil temperature, *in situ* water content, SOM, NH_4^+, activities of AG, BX, CEL, and POX, bacterial biomass, bacterial and fungal abundance, and *nos*Z gene abundance ($P<0.05$, Supplementary Fig. S5). There were no significant correlations between CH_4 fluxes and soil and microbial variables across all sites (Supplementary Fig. S4), and above (Supplementary Fig. S5) or below the treeline (except for the positive correlations with fungal biomass and *nos*Z gene abundance, Supplementary Fig. S6). Additionally, activities of all eight enzymes were significantly correlated to 16S rRNA gene copies ($P<0.05$).

Using three types of models (SEM, HP and RF), we successfully predicted direct and indirect effects of environmental factors on microbial activities and fluxes of CO_2, CH_4 and N_2O (Fig. 8).

SEM analysis (Fig. 8A) showed that air MAT, A/T ratio (OM composition, the higher A/T ratio, the more humic-like OM is), and C-acquiring enzyme activities were significantly and directly controlling CO_2 fluxes (all $P<0.05$). Enzyme activities were significantly influenced by both SOM quantity and composition. OM quantity, influenced by air MAT, had a significant influence on OM composition. HP analysis (Fig. 8A) confirmed the significant contributions of air MAT and OM quantity and composition to CO_2 fluxes (10.7 %, 8.7 %, and 8.5 %, respectively; $P<0.05$). Additionally, C/N ratio, 16S rRNA gene abundance, and PO_4^{3-} contributed significantly to CO_2 fluxes (31.1 %, 19.2 %, and 11.1 %, respectively; $P<0.05$). RF regression (Fig. 8A) showed that air MAT, C/N ratio, PO_4^{3-}, bacterial abundance and biomass, fungal abundance, and OM composition with the FI and HIX indices, SOM, MAP, 16S rRNA and *pho*D gene abundance, and NAG enzyme were of great importance (over 4.0 % individually, over 70.0 % in total) to the variations in CO_2 fluxes.

No significant influence of functional genes *mcr*A and *pmo*A on CH_4 fluxes was observed in the three models (Fig. 8B). However, CH_4 fluxes were negatively related to A/T ratio (SEM, $P<0.01$). HP also confirmed that CH_4 fluxes were significantly influenced by OM composition (A/T ratio, 30.9 %, $P<0.05$, Fig. 8B). Additionally, RF regression (Fig. 8B) showed that C-acquiring enzymes of CEL and BX, air MAT, pH, fungal biomass, OM composition (HIX and A/T ratio), LAP enzyme, NH_4^+, and C/N ratio had a high influence on CH_4 fluxes (over 70.0 % importance in total).

N_2O fluxes were significantly controlled by the abundance of *nor*B gene encoded for N_2O production, which was significantly controlled by air MAT, and OM quantity and composition (SEM, $P<0.05$, Fig. 8C). Despite of nonsignificant contributions from any of the variables based on HP, functional genes abundances of *nor*B (18.4 %), archaeal *amo*A (17.5 %) and *nos*Z (16.9 %), air MAT (15.0 %) and N-acquiring enzymes of LAP (10.9 %) and NAG (7.0 %), influenced N_2O fluxes the most (Fig. 8C). Similarly, RF regressions also indicated that the most influential variables were gene abundances of archaeal and bacterial *amo*A, *nor*B, NO_3^-, *pho*D, *nos*Z, TN, C-acquiring enzymes of BX and AG, pH,

phosphatase, A/T ratio, and bacterial gene abundance and biomass (over 70.0 % importance in total, Fig. 8C).

4. Discussion

4.1. The treeline is a demarcation point for elevational changes in GHG fluxes, microbial activities, soil properties and OM composition

Our results clearly show that the treeline is a demarcation point along alpine elevational gradients. GHG fluxes, especially CO_2 and N_2O fluxes, exhibited differential patterns below and above the treeline. CO_2 fluxes exhibited a hump-shaped elevational pattern, slightly increasing from low altitudinal temperate to the subalpine forests and decreasing from the treeline to the mountain summit, as were similarly observed for C-acquiring enzymes (AG, BX, CEL and POX), and bacterial and fungal biomass and gene abundances. Similar soil respiration patterns were also observed in the Dongling mountains, China, where microbial functions and soil nutrients variations also followed the vegetation transition (Shen et al., 2021). While N_2O fluxes, mostly negative (N_2O uptake), stayed stable across the forest sites, they increased significantly from the treeline to the mountain summit. While there were no significant changes of N-acquiring enzymes (NAG and LAP) below or above the treeline, decreases in the abundances of *nor*B (N_2O production) and *nos*Z (N_2O reduction) genes were clearly observed from the treeline to the summit. Contrastingly, no significant changes of CH_4 fluxes were found along the altitudinal gradient, neither were detected in the microbial functional genes encoded for CH_4 production or oxidation. Similar patterns of CH_4 fluxes were also observed in montane forest soils along an elevational gradient in tropical Peruvian Andes (Teh et al., 2014) and the Qinling Mountains, China (Pang et al., 2023).

Similar to GHG fluxes, soil properties, i.e., soil *in situ* gravimetric water content, SOM, TOC, TN, C/N ratio, nutrients (NH_4^+ and PO_4^{3-}), and OM composition indices, remained steady or slightly increased from the low altitudinal temperate to the subalpine forests near the treeline but decreased from the treeline to the mountain summit. The reduced soil water content from the treeline to the mountain summit might be associated with a lower water holding capacity of shallower soils and limited plant cover from forests towards higher altitudinal soils (Jasper et al., 2006; Rime et al., 2015). The significant decreases in SOM, TOC, TN, C/N ratio, and nutrients from the treeline to the summit are also likely to be attributed to the decreased contribution of plant detritus (e.g. by trees and grasses) (Devos et al., 2022; Kammer et al., 2009; Muller et al., 2017), which is in accordance with the significantly reduced litter biomass collected at the soil surface from the treeline to the mountain summit (Supplementary Fig. S7). In contrast, the increased content of SOM, TOC, TN, and C/N ratio were observed from the low altitudinal temperate forests to the subalpine forests close to the treeline. These have been corroborated from mixed deciduous forests to coniferous forests with increasing elevation, with high altitudinal soils containing higher amount of SOM and nutrients from coniferous litter (Berger et al., 2015; Siles et al., 2017; Siles et al., 2016; Whitaker et al., 2014). Increasing HIX and A/T and C/T peak ratios of the WEOM extracts indicates an increased humification of SOM with increasing elevation below the treeline. Moreover, increasing BIX and FI values of the WEOM extracts, together with a decrease in HIX and A/T and C/T peak ratios, indicates a gradual shift from soils dominated by plant-derived humic OM close to the treeline to protein-like OM of microbial origin further towards the summit.

4.2. SOM quantity and composition as drivers of microbial enzyme activities and GHG fluxes

Significant contributions of environmental variables, e.g., air MAT, MAP, SOM quantity and composition, C/N ratio and nutrients (PO_4^{3-}) to regulating microbial enzyme activities and CO_2 fluxes based on correlations and on the different tested models were found along the elevational gradient. Soil temperature and moisture have been widely observed to play a fundamental role in promoting soil respiration in temperate montane forest soils along an elevational gradient (Badraghi et al., 2021; Pang et al., 2023; Rodeghiero & Cescatti, 2005). Besides microbial respiration from OC, root respiration may contribute to CO_2 emissions from our soils. However, we expect this contribution to be minor, as root respiration can only account for 10 % of the total soil respiration (Hanson et al., 2000). SOM quantity, maximizing in the subalpine forests close to the treeline, was positively correlated to C-acquiring enzyme activities. At higher elevation, low temperatures generally limit the decomposition of SOM by reducing microbial activities, which causes a greater amount of SOM to accumulate (de la Cruz-Amo et al., 2020; Prietzel et al., 2016). Likewise, a higher humification degree of SOM with increased SOM quantity was also found in other mountain forests (Siles et al., 2017; Siles et al., 2016). Yet, the enlarged amount of SOM stocks at higher elevation potentially increases microbial biomass and respiration, due to more fresh C and nutrients (N and P) inputs from SOM in spite of lower temperatures (He et al., 2016; Siles et al., 2017; Siles et al., 2016; Whitaker et al., 2014). This mechanism is in accordance with the observed increase in microbial biomass and SOM quantity together with increased CO_2 fluxes from the low-altitudinal to the subalpine forests. Soil C:N ratio was also significantly correlated to SOM quantity, C-acquiring enzymes and CO_2 fluxes, as was previously reported (Li et al., 2022). Yet, our results are contradictory to the established knowledge that a lower C/N ratio favors SOM decomposition by providing more available N to microbes (Hu et al., 2001). Instead, our results suggest that increasing amounts of soil N and OM from low-altitudinal to subalpine forests provide more available N and decomposable C to the microorganisms, whose activities enhanced the decomposition rate of SOM and CO_2 emissions (Li et al., 2022; Pang et al., 2023). Moreover, SOM composition (SOM humification indicated by A/T ratio) was significantly and positively associated with SOM quantity, C/N ratio, microbial biomass, and CO_2 fluxes. While the SOM quantity and composition (humification indicated by A/T ratio) index, and nutrients increased with the elevation, an increasing amount of fresh C and N is available to microbes for growth and activities, causing the higher CO_2 fluxes observed at higher elevation forest sites. Above the treeline, air MAT, soil *in situ* temperature, SOM quantity and contribution of plant derived OM (humid OM), and nutrients decreased dramatically, lowering microbial activities, SOM decomposition and CO_2 fluxes.

The soils studied along the elevational gradient were all CH_4 sinks (more CH_4 oxidation than CH_4 production), which is in line with previously documented CH_4 measurements in montane forest and grassland soils, both soil types being CH_4 sinks (Imer et al., 2013; Martinson et al., 2021; Pang et al., 2023; Wolf et al., 2012). SOM composition (higher A/T ratio) contributed negatively to CH_4 fluxes. With the increase in A/T ratio with the elevation, SOM became more humic, and therefore less C was available for CH_4 production (Megonigal & Guenther, 2008). Soil CH_4 fluxes result from the balance of CH_4 production and consumption, driven by methanogens and methanotrophs (Conrad, 2009). However, we did not find a correlation between methanogenic *mcr*A and methanotrophic *pmo*A genes abundance and CH_4 fluxes along the elevational gradient.

N_2O fluxes, which were mostly negative along the whole elevation gradient (N_2O uptake in the soil), were driven by abundances of functional genes *amo*A (ammonia oxidation) and *nor*B (N_2O production), which were controlled by air MAT, soil *in situ* water content, SOM quantity and composition. Soil N_2O fluxes are the balance of N_2O production and consumption by denitrifiers (Chapuis-Lardy et al., 2007). *amo*A and the denitrification substance NO_3^- were both significantly depressed by the humification of SOM (higher A/T ratio), which indicated a decreased rate of nitrification. Furthermore, the observed low archaeal *amo*A gene abundance below the treeeline might indicate a paucity of substrate needed for the denitrification (NO_3^-) and the production of N_2O production, causing a N_2O sink. Denitrifying gene *nor*B

could be promoted by soil temperature and moisture, which provide more anaerobic conditions, a prerequisite for denitrification (Ruser et al., 2006; Trost et al., 2013). Nevertheless, while *nor*B gene abundance was positively impacted by air MAT and soil *in situ* water content, it was suppressed by both SOM quantity and quality (higher A/T ratio, less available to denitrifiers) according to SEM model. Therefore, the limitation of the *nor*B gene potentially caused an increase of N_2O uptake in the soils along the whole elevation gradient. Similar negative associations of microbially unavailable (recalcitrant) OM with N_2O production (denitrification) was also observed in other soil ecosystems (Pare & Bedard-Haughn, 2013). Above the treeline, there was a negative correlation between N_2O fluxes and *nos*Z gene abundance, and the reduced *nos*Z gene abundance from the treeline site to the summit potentially lowered N_2O consumption rate by microbial cells.

Overall, higher values of SOM quantity and composition indices contributed significantly to the increased soil respiration and atmospheric N_2O uptake along the elevational gradient. However, it should be noted that GHG fluxes, similar to the other microbial and environmental parameters, were measured once at each site, which might have limited the comparison to parameters representing soil processes developing over longer time-scales, such as SOM quantity and quality. Data from repetitive measurements of GHG fluxes, for example, cross seasons or even years, could potentially improve the comparison of GHG fluxes with microbial and soil parameters.

4.3. Expected alteration of GHG fluxes with the upward shift of the treeline as a consequence of global change

Alpine regions are vulnerable to rapid climate change and are expected to undergo an increase in their mean annual temperatures by 1.0 – 4.0 °C by 2070 – 2099 compared to those in 1981–2010 (Kotlarski et al., 2023). Treelines on mountains have been predicted to shift upwards with increased temperatures under global change (Du et al., 2018; Körner, 2012), along with forests colonizing Alpine meadows and grasses colonizing the barren soils on mountain summits (Du et al., 2018; Hagedorn et al., 2014). Litter input from newly colonizing trees and grasses to soils at the higher elevation will cause more entry of OM (C and nutrients) into the soils, providing more available substrates for microbial activities, such as C-acquiring enzyme activities, and for microbial biomass C (Kammer et al., 2009). Additionally, due to the increased input of terrestrial derived OM, previously microbial-derived OM dominated soils will become more humic-like OM dominating, as is inferred by higher OM compositional A/T ratio in the subalpine forest soils. These together, imply the increases in microbial activities, biomass, and CO_2 emissions in high-elevational mountain soils with the treeline moving upwards in predicted near-future climates. As treeline tends to move upward, it is probable that soils at high elevation (above the treeline) switch from a N_2O source to a sink, as SOM quantity and humification degree is expected to increase with the colonization of trees. However, considering the absence of significant changes of CH_4 fluxes along the elevation gradient, soils at higher elevation will likely continue to serve as CH_4 sinks in the near future. Such projections may provide new insights into the global climate change models in terrestrial ecosystems, especially in mountain soils. Considering the interplay between edaphic parameters, microbial enzyme sactivities, and GHG fluxes for both below and above the treeline might help to better predict soil C stocks, gains, and losses in response to future global climate change.

5. Conclusion

Our study showed significant changes of CO_2 fluxes along the elevation gradient, displaying a hump-shaped relationship with increasing elevation and maximizing before the treeline and declining towards the summit. The fluxes were controlled by microbial enzyme activities and further by air MAT, and SOM quantity and composition (the proportion of plant derived humic-like vs. protein-like OM). Despite of a nonsignificant pattern along the elevation, CH_4 fluxes were dominated by net uptake of atmospheric CH_4 and were mostly controlled by SOM composition, though not related to methane cycling genes. A stable uptake of atmospheric N_2O was observed below the treeline, followed by a significant decrease from the treeline to the summit, which was driven by specific nitrifying (*amo*A) and denitrifying (*nor*B) genes and further by air MAT and SOM quantity and composition.

Author contributions

AF and XH designed the study and conducted the field measurements and sampling. XH conducted the lab work with the help of ADP, JPCR, AMR (extracellular enzyme activities, microbial biomass and SOM composition measurements), JD, and AP (DNA extraction). XH analyzed the data and wrote the manuscript with input from all co-authors. The final version has been revised and approved by all authors.

CRediT authorship contribution statement

Xingguo Han: Writing – review & editing, Writing – original draft, Methodology, Formal analysis, Data curation, Conceptualization. **Anna Doménech-Pascual:** Writing – review & editing, Methodology. **Joan Pere Casas-Ruiz:** Writing – review & editing, Methodology. **Jonathan Donhauser:** Writing – review & editing, Methodology. **Karen Jordaan:** Writing – review & editing, Methodology. **Jean-Baptiste Ramond:** Writing – review & editing, Funding acquisition. **Anders Priemé:** Writing – review & editing, Funding acquisition. **Anna M. Romaní:** Writing – review & editing, Funding acquisition. **Aline Frossard:** Writing – review & editing, Supervision, Funding acquisition, Conceptualization.

Declaration of competing interest

The authors declare that they have no known competing financial interests or personal relationships that could have appeared to influence the work reported in this paper.

Data availability

Data will be made available on request.

Acknowledgements

The authors thank the Swiss National Park and Biosfera Val Müstair for field access. The authors further acknowledge Laura Medici for help on the field and in the lab at WSL, Joan Ferriol-Ciurana at the University of Girona for conducting extracellular enzyme assays, George Stoletov at the University of Copenhagen for extracting the DNA and Dr. Jörg Luster, Daniel Christen and Roger Köchli at WSL for their assistance for the soil physico-chemical properties. The authors also thank the Swiss Long-term Forest Ecosystem Research programme LWF for field access and climatic data. This study was funded by the Swiss National Science Foundation (SNF 31BD30_193667), the Spanish State Research Agency (PCI2020-120702-2/AEI/10.13039/501100011033), the Innovation Fund Denmark (BiodivClim-76 GRADCATCH), and the Department of Science and Innovation of the Republic of South Africa (GRADCATCH), through the 2019-2020 BiodivERsA joint call for research proposals, under the BiodivClim ERA-Net COFUND programme.

Appendix A. Supplementary data

Supplementary data to this article can be found online at https://doi.org/10.1016/j.geoderma.2024.116993.

References

Amalfitano, S., Fazi, S., 2008. Recovery and quantification of bacterial cells associated with streambed sediments. J. Microbiol. Methods 75 (2), 237–243. https://doi.org/10.1016/j.mimet.2008.06.004.

Badraghi, A., Ventura, M., Polo, A., Borruso, L., Giammarchi, F., Montagnani, L., 2021. Soil respiration variation along an altitudinal gradient in the Italian Alps: Disentangling forest structure and temperature effects. PLoS One 16 (8). https://doi.org/10.1371/journal.pone.0247893.

Bardelli, T., Gomez-Brandon, M., Ascher-Jenull, J., Fornasier, F., Arfaioli, P., Francioli, D., Pietramellara, G., 2017. Effects of slope exposure on soil physico-chemical and microbiological properties along an altitudinal climosequence in the Italian Alps. Sci. Total Environ. 575, 1041–1055. https://doi.org/10.1016/j.scitotenv.2016.09.176.

Barry, R.G., 2008. Geographical controls of mountain meteorological elements. In: Barry, R.G. (Ed.), Mountain Weather and Climate. Cambridge University Press, Cambridge, pp. 24–124.

Berger, T.W., Duboc, O., Djukic, I., Tatzber, M., Gerzabek, M.H., Zehetner, F., 2015. Decomposition of beech (Fagus sylvatica) and pine (Pinus nigra) litter along an Alpine elevation gradient: Decay and nutrient release. Geoderma 251, 92–104. https://doi.org/10.1016/j.geoderma.2015.03.024.

Bratbak, G., Dundas, I., 1984. Bacterial dry-matter content and biomass estimations. Appl. Environ. Microbiol. 48 (4), 755–757. https://doi.org/10.1128/Aem.48.4.755-757.1984.

Breiman, L., 2001. Random forests. Mach. Learn. 45 (1), 5–32. https://doi.org/10.1023/A:1010933404324.

Butterbach-Bahl, K., Baggs, E.M., Dannenmann, M., Kiese, R., Zechmeister-Boltenstern, S., 2013. Nitrous oxide emissions from soils: how well do we understand the processes and their controls? Philosoph. Trans. Royal Soc. B-Biol. Sci. 368 (1621) https://doi.org/10.1098/rstb.2013.0122.

Chantigny, M.H., Harrison-Kirk, T., Curtin, D., Beare, M., 2014. Temperature and duration of extraction affect the biochemical composition of soil water-extractable organic matter. Soil Biol. Biochem. 75, 161–166. https://doi.org/10.1016/j.soilbio.2014.04.011.

Chapuis-Lardy, L., Wrage, N., Metay, A., Chotte, J.L., Bernoux, M., 2007. Soils, a sink for N2O? A review. Global Change Biol. 13 (1), 1–17. https://doi.org/10.1111/j.1365-2486.2006.01280.x.

Conrad, R., 2009. The global methane cycle: recent advances in understanding the microbial processes involved. Environ. Microbiol. Rep. 1 (5), 285–292. https://doi.org/10.1111/j.1758-2229.2009.00038.x.

Davidson, E.A., Janssens, I.A., 2006. Temperature sensitivity of soil carbon decomposition and feedbacks to climate change. Nature 440 (7081), 165–173. https://doi.org/10.1038/nature04514.

Davies, B.E., 1974. Loss-on-ignition as an estimate of soil organic-matter. Soil Sci. Soc. Am. J. 38 (1), 150–151. https://doi.org/10.2136/sssaj1974.03615995003800010046x.

de la Cruz-Amo, L., Banares-de-Dios, G., Cala, V., Granzow-de la Cerda, I.G., Espinosa, C. I., Ledo, A., Cayuela, L., 2020. Trade-offs among aboveground, belowground, and soil organic carbon stocks along altitudinal gradients in andean tropical montane forests. Front. Plant Sci. 11 https://doi.org/10.3389/fpls.2020.00106.

Devos, C.C., Ohlson, M., Naesset, E., Bollandsas, O.M., 2022. Soil carbon stocks in forest-tundra ecotones along a 500 km latitudinal gradient in northern Norway. Sci. Rep. 12 (1) https://doi.org/10.1038/s41598-022-17409-3.

Donhauser, J., Frey, B., 2018. Alpine soil microbial ecology in a changing world. FEMS Microbiol. Ecol. 94 (9) https://doi.org/10.1093/femsec/fiy099.

Du, H.B., Liu, J., Li, M.H., Büntgen, U., Yang, Y., Wang, L., He, H.S., 2018. Warming-induced upward migration of the alpine treeline in the Changbai Mountains, northeast China. Glob. Chang. Biol. 24 (3), 1256–1266. https://doi.org/10.1111/gcb.13963.

Dutaur, L., Verchot, L.V., 2007. A global inventory of the soil CH(4) sink. Global Biogeochem. Cycles 21 (4). https://doi.org/10.1029/2006gb002734.

Fatumah, N., Munishi, L.K., Ndakidemi, P.A., 2019. Variations in greenhouse gas fluxes in response to short-term changes in weather variables at three elevation ranges, Wakiso District, Uganda. Atmosphere 10 (11). https://doi.org/10.3390/atmos10110708.

Fellman, J.B., Hood, E., Spencer, R.G.M., 2010. Fluorescence spectroscopy opens new windows into dissolved organic matter dynamics in freshwater ecosystems: A review. Limnol. Oceanogr. 55 (6), 2452–2462. https://doi.org/10.4319/lo.2010.55.6.2452.

Fuss, R., Hueppi, R., & Pedersen, A. R. (2015). R-Package: Gasfluxes.

Gardner, C.M., Robinson, D., Blyth, K., Cooper, J.D., 2000. Soil water content. In: Soil and Environmental Analysis. CRC Press, pp. 13–76.

Gee, G.W., Bauder, J.W., 1986. Particle-size analysis. Methods Soil Anal. Part 1. Phys. Mineral. Methods 5, 383–411.

Gessner, M.O., 2005. Ergosterol as a measure of fungal biomass. Methods Study Litt. Decomposit. A Pract. Guide 189–196.

Gessner, M.O., Chauvet, E., 1993. Ergosterol-to-biomass conversion factors for aquatic hyphomycetes. Appl. Environ. Microbiol. 59 (2), 502–507. https://doi.org/10.1128/Aem.59.2.502-507.1993.

Goldberg, S.D., Gebauer, G., 2009. N2O and NO fluxes between a Norway spruce forest soil and atmosphere as affected by prolonged summer drought. Soil Biol. Biochem. 41 (9), 1986–1995. https://doi.org/10.1016/j.soilbio.2009.07.001.

Hagedorn, F., Joos, O., 2014. Experimental summer drought reduces soil CO2 effluxes and DOC leaching in Swiss grassland soils along an elevational gradient. Biogeochemistry 117 (2–3), 395–412. https://doi.org/10.1007/s10533-013-9881-x.

Hagedorn, F., Shiyatov, S.G., Mazepa, V.S., Devi, N.M., Grigor'ev, A.A., Bartysh, A.A., Moiseev, P.A., 2014. Treeline advances along the Urals mountain range - driven by improved winter conditions? Glob. Chang. Biol. 20 (11), 3530–3543. https://doi.org/10.1111/gcb.12613.

Han, X., Beck, K., Bürgmann, H., Frey, B., Stierli, B., Frossard, A., 2023. Synthetic oligonucleotides as quantitative PCR standards for quantifying microbial genes. Front. Microbiol. 14 https://doi.org/10.3389/fmicb.2023.1279041.

Hansen, A.M., Kraus, T.E.C., Pellerin, B.A., Fleck, J.A., Downing, B.D., Bergamaschi, B.A., 2016. Optical properties of dissolved organic matter (DOM): Effects of biological and photolytic degradation. Limnol. Oceanogr. 61 (3), 1015–1032. https://doi.org/10.1002/lno.10270.

Hanson, P.J., Edwards, N.T., Garten, C.T., Andrews, J.A., 2000. Separating root and soil microbial contributions to soil respiration: A review of methods and observations. Biogeochemistry 48 (1), 115–146. https://doi.org/10.1023/A:1006244819642.

Harrell Jr, F. E., & Harrell Jr, M. F. E. (2019). Package 'hmisc'. *CRAN2018*, 235-236.

He, X.J., Hou, E.Q., Liu, Y., Wen, D.Z., 2016. Altitudinal patterns and controls of plant and soil nutrient concentrations and stoichiometry in subtropical China. Sci. Rep. 6 https://doi.org/10.1038/srep24261.

He, X.J., Hou, E.Q., Veen, G.F., Ellwood, M.D.F., Dijkstra, P., Sui, X.H., Chu, C.J., 2020. Soil microbial biomass increases along elevational gradients in the tropics and subtropics but not elsewhere. Glob. Ecol. Biogeogr. 29 (2), 345–354. https://doi.org/10.1111/geb.13017.

Hu, S., Chapin, F.S., Firestone, M.K., Field, C.B., Chiariello, N.R., 2001. Nitrogen limitation of microbial decomposition in a grassland under elevated CO. Nature 409 (6817), 188–191. https://doi.org/10.1038/35051576.

Huguet, A., Vacher, L., Relexans, S., Saubusse, S., Froidefond, J.M., Parlanti, E., 2009. Properties of fluorescent dissolved organic matter in the Gironde Estuary. Org Geochem. 40 (6), 706–719. https://doi.org/10.1016/j.orggeochem.2009.03.002.

Imer, D., Merbold, L., Eugster, W., Buchmann, N., 2013. Temporal and spatial variations of soil CO2, CH4 and N2O fluxes at three differently managed grasslands. Biogeosciences 10 (9), 5931–5945. https://doi.org/10.5194/bg-10-5931-2013.

IPCC. (2014). Synthesis Report. Contribution of working groups I." II and III to the fifth assessment report of the intergovernmental panel on climate change.

Janssens, I.A., Lankreijer, H., Matteucci, G., Kowalski, A.S., Buchmann, N., Epron, D., Valentini, R., 2001. Productivity overshadows temperature in determining soil and ecosystem respiration across European forests. Glob. Chang. Biol. 7 (3), 269–278. https://doi.org/10.1046/j.1365-2486.2001.00412.x.

Jasper, K., Calanca, P., Fuhrer, J., 2006. Changes in summertime soil water patterns in complex terrain due to climatic change. J. Hydrol. 327 (3–4), 550–563. https://doi.org/10.1016/j.jhydrol.2005.11.061.

Kammer, A., Hagedorn, F., Shevchenko, I., Leifeld, J., Guggenberger, G., Goryacheva, T., Moiseev, P., 2009. Treeline shifts in the Ural mountains affect soil organic matter dynamics. Glob. Chang. Biol. 15 (6), 1570–1583. https://doi.org/10.1111/j.1365-2486.2009.01856.x.

Kobler, J., Zehetgruber, B., Dirnböck, T., Jandl, R., Mirtl, M., Schindlbacher, A., 2019. Effects of aspect and altitude on carbon cycling processes in a temperate mountain forest catchment. Landsc. Ecol. 34 (2), 325–340. https://doi.org/10.1007/s10980-019-00769-z.

Körner, C., 2012. Alpine Treelines: Functional Ecology of the Global High Elevation Tree Limits. Springer Science & Business Media, Basel.

Kotlarski, S., Gobiet, A., Morin, S., Olefs, M., Rajczak, J., Samacoïts, R., 2023. 21st Century alpine climate change. Clim. Dyn. 60 (1–2), 65–86. https://doi.org/10.1007/s00382-022-06303-3.

Kuo, S., 1996. Phosphorus. In: Sparks, D.L. (Ed.), Methods of Soil Analysis, Part 3: Chemical Methods, SSSA Book Series, pp. 869–919.

Lai, T.V., Denton, M.D., 2018. N2O and N2 emissions from denitrification respond differently to temperature and nitrogen supply. J. Soil. Sediment. 18 (4), 1548–1557. https://doi.org/10.1007/s11368-017-1863-5.

Lazcano, C., Zhu-Barker, X., Decock, C., 2021. Effects of organic fertilizers on the soil microorganisms responsible for N2O emissions: A review. Microorganisms 9 (5). https://doi.org/10.3390/microorganisms9050983.

Lefcheck, J.S., 2016. piecewiseSEM: Piecewise structural equation modelling in R for ecology, evolution, and systematics. Methods Ecol. Evol. 7 (5), 573–579. https://doi.org/10.1111/2041-210x.12512.

Li, C., Xiao, C.W., Li, M.X., Xu, L., He, N.P., 2022. A global synthesis of patterns in soil organic matter and temperature sensitivity along the altitudinal gradient. Front. Environ. Sci. 10 https://doi.org/10.3389/fenvs.2022.959292.

Looby, C.I., Martin, P.H., 2020. Diversity and function of soil microbes on montane gradients: the state of knowledge in a changing world. FEMS Microbiol. Ecol. 96 (9) https://doi.org/10.1093/femsec/fiaa122.

Lu, Y.H., Wassmann, R., Neue, H.U., Huang, C.Y., 2000. Dynamics of dissolved organic carbon and methane emissions in a flooded rice soil. Soil Sci. Soc. Am. J. 64 (6), 2011–2017. https://doi.org/10.2136/sssaj2000.6462011x.

Ludwig, J., Meixner, F.X., Vogel, B., Forstner, J., 2001. Soil-air exchange of nitric oxide: An overview of processes, environmental factors, and modeling studies. Biogeochemistry 52 (3), 225–257. https://doi.org/10.1023/A:1006424330555.

Ma, M.Z., Zang, Z.H., Xie, Z.Q., Chen, Q.S., Xu, W.T., Zhao, C.M., Shen, G.Z., 2019. Soil respiration of four forests along elevation gradient in northern subtropical China. Ecol. Evol. 9 (22), 12846–12857. https://doi.org/10.1002/ece3.5762.

Mac Nally, R., 1996. Hierarchical partitioning as an interpretative tool in multivariate inference. Aust. J. Ecol. 21 (2), 224–228. https://doi.org/10.1111/j.1442-9993.1996.tb00602.x.

Mac Nally, R., 2002. Multiple regression and inference in ecology and conservation biology: further comments on identifying important predictor variables. Biodivers. Conserv. 11 (8), 1397–1401. https://doi.org/10.1023/A:1016250716679.

Mac Nally, R., Walsh, C.J., 2004. Hierarchical partitioning public-domain software. Biodivers. Conserv. 13 (3), 659–660.
Martinson, G.O., Corre, M.D., Veldkamp, E., 2013. Responses of nitrous oxide fluxes and soil nitrogen cycling to nutrient additions in montane forests along an elevation gradient in southern Ecuador. Biogeochemistry 112 (1–3), 625–636. https://doi.org/10.1007/s10533-012-9753-9.
Martinson, G.O., Muller, A.K., Matson, A.L., Corre, M.D., Veldkamp, E., 2021. Nitrogen and phosphorus control soil methane uptake in tropical montane forests. J. Geophys. Res.-Biogeosci. 126 (8) https://doi.org/10.1029/2020JG005970.
McKnight, D.M., Boyer, E.W., Westerhoff, P.K., Doran, P.T., Kulbe, T., Andersen, D.T., 2001. Spectrofluorometric characterization of dissolved organic matter for indication of precursor organic material and aromaticity. Limnol. Oceanogr. 46 (1), 38–48. https://doi.org/10.4319/lo.2001.46.1.0038.
Megonigal, J.P., Guenther, A.B., 2008. Methane emissions from upland forest soils and vegetation. Tree Physiol. 28 (4), 491–498. https://doi.org/10.1093/treephys/28.4.491.
Melillo, J.M., Frey, S.D., DeAngelis, K.M., Werner, W.J., Bernard, M.J., Bowles, F.P., Grandy, A.S., 2017. Long-term pattern and magnitude of soil carbon feedback to the climate system in a warming world. Science 358 (6359), 101–104. https://doi.org/10.1126/science.aan2874.
Müller, A.K., Matson, A.L., Corre, M.D., Veldkamp, E., 2016. Soil N2O fluxes along an elevation gradient of tropical montane forests under experimental nitrogen and phosphorus addition. Front. Earth Sci. 3, 66. https://doi.org/10.3389/feart.2015.00066.
Muller, M., Oelmann, Y., Schickhoff, U., Bohner, J., Scholten, T., 2017. Himalayan treeline soil and foliar C:N: P stoichiometry indicate nutrient shortage with elevation. Geoderma 291, 21–32. https://doi.org/10.1016/j.geoderma.2016.12.015.
Neto, E.S., Carmo, J.B., Keller, M., Martins, S.C., Alves, L.F., Vieira, S.A., Martinelli, L.A., 2011. Soil-atmosphere exchange of nitrous oxide, methane and carbon dioxide in a gradient of elevation in the coastal Brazilian Atlantic forest. Biogeosciences 8 (3), 733–742. https://doi.org/10.5194/bg-8-733-2011.
Oertel, C., Matschullat, J., Zurba, K., Zimmermann, F., Erasmi, S., 2016. Greenhouse gas emissions from soils A review. Chem. Erde-Geochem. 76 (3), 327–352. https://doi.org/10.1016/j.chemer.2016.04.002.
Orchard, V.A., Cook, F.J., 1983. Relationship between Soil Respiration and Soil-Moisture. Soil Biol. Biochem. 15 (4), 447–453. https://doi.org/10.1016/0038-0717(83)90010-X.
Pang, J.Z., Peng, C.H., Wang, X.K., Zhang, H.X., Zhang, S.X., 2023. Soil-atmosphere exchange of carbon dioxide, methane and nitrous oxide in temperate forests along an elevation gradient in the Qinling Mountains, China. Plant and Soil. https://doi.org/10.1007/s11104-023-05967-y.
Pare, M.C., Bedard-Haughn, A., 2013. Soil organic matter quality influences mineralization and GHG emissions in cryosols: a field-based study of sub- to high Arctic. Glob. Chang. Biol. 19 (4), 1126–1140. https://doi.org/10.1111/gcb.12125.
Pind, A., Freeman, C., Lock, M.A., 1994. Enzymic degradation of phenolic materials in peatlands—measurement of phenol oxidase activity. Plant and Soil 159 (2), 227–231.
Pries, C.E.H., Castanha, C., Porras, R.C., Torn, M.S., 2017. The whole-soil carbon flux in response to warming. Science 355 (6332), 1420–1422. https://doi.org/10.1126/science.aal1319.
Prietzel, J., Zimmermann, L., Schubert, A., Christophel, D., 2016. Organic matter losses in German Alps forest soils since the 1970s most likely caused by warming. Nat. Geosci. 9 (7), 543–548. https://doi.org/10.1038/Ngeo2732.
Purbopuspito, J., Veldkamp, E., Brumme, R., Murdiyarso, D., 2006. Trace gas fluxes and nitrogen cycling along an elevation sequence of tropical montane forests in Central Sulawesi, Indonesia. Global Biogeochem. Cycles 20 (3). https://doi.org/10.1029/2005gb002516.
Rime, T., Hartmann, M., Brunner, I., Widmer, F., Zeyer, J., Frey, B., 2015. Vertical distribution of the soil microbiota along a successional gradient in a glacier forefield. Mol. Ecol. 24 (5), 1091–1108. https://doi.org/10.1111/mec.13051.
Rodeghiero, M., Cescatti, A., 2005. Main determinants of forest soil respiration along an elevation/temperature gradient in the Italian Alps. Glob. Chang. Biol. 11 (7), 1024–1041. https://doi.org/10.1111/j.1365-2486.2005.00963.x.
Ruser, R., Flessa, H., Russow, R., Schmidt, G., Buegger, F., Munch, J.C., 2006. Emission of N2O, N-2 and CO2 from soil fertilized with nitrate: Effect of compaction, soil moisture and rewetting. Soil Biol. Biochem. 38 (2), 263–274. https://doi.org/10.1016/j.soilbio.2005.05.005.
Schmidt, M.W.I., Torn, M.S., Abiven, S., Dittmar, T., Guggenberger, G., Janssens, I.A., Trumbore, S.E., 2011. Persistence of soil organic matter as an ecosystem property. Nature 478 (7367), 49–56. https://doi.org/10.1038/nature10386.
Shen, C.C., He, J.Z., Ge, Y., 2021. Seasonal dynamics of soil microbial diversity and functions along elevations across the treeline. Sci. Total Environ. 794 https://doi.org/10.1016/j.scitotenv.2021.148644.
Siles, J.A., Cajthaml, T., Minerbi, S., Margesin, R., 2016. Effect of altitude and season on microbial activity, abundance and community structure in Alpine forest soils. FEMS Microbiol. Ecol. 92 (3) https://doi.org/10.1093/femsec/fiw008.
Siles, J.A., Cajthaml, T., Filipova, A., Minerbi, S., Margesin, R., 2017. Altitudinal, seasonal and interannual shifts in microbial communities and chemical composition of soil organic matter in Alpine forest soils. Soil Biol. Biochem. 112, 1–13. https://doi.org/10.1016/j.soilbio.2017.04.014.
Siles, J.A., Margesin, R., 2016. Abundance and diversity of bacterial, archaeal, and fungal communities along an altitudinal gradient in alpine forest soils: what are the driving factors? Microb. Ecol. 72 (1), 207–220. https://doi.org/10.1007/s00248-016-0748-2.
Smith, K.A., Dobbie, K.E., Ball, B.C., Bakken, L.R., Sitaula, B.K., Hansen, S., Orlanski, P., 2000. Oxidation of atmospheric methane in Northern European soils, comparison with other ecosystems, and uncertainties in the global terrestrial sink. Glob. Chang. Biol. 6 (7), 791–803. https://doi.org/10.1046/j.1365-2486.2000.00356.x.
Smith, K.A., Ball, T., Conen, F., Dobbie, K.E., Massheder, J., Rey, A., 2003. Exchange of greenhouse gases between soil and atmosphere: interactions of soil physical factors and biological processes. Eur. J. Soil Sci. 54 (4), 779–791. https://doi.org/10.1046/j.1351-0754.2003.0567.x.
Stocker, T., 2014. Climate change 2013: the physical science basis: Working Group I contribution to the Fifth assessment report of the Intergovernmental Panel on Climate Change. Cambridge University Press.
Teh, Y.A., Diem, T., Jones, S., Quispe, L.P.H., Baggs, E., Morley, N., Meir, P., 2014. Methane and nitrous oxide fluxes across an elevation gradient in the tropical Peruvian Andes. Biogeosciences 11 (8), 2325–2339. https://doi.org/10.5194/bg-11-2325-2014.
Theil-Nielsen, J., Sondergaard, M., 1998. Bacterial carbon biomass calculated from biovolumes. Arch. Hydrobiol. 141 (2), 195–207. https://doi.org/10.1127/archiv-hydrobiol/141/1998/195.
Trost, B., Prochnow, A., Drastig, K., Meyer-Aurich, A., Ellmer, F., Baumecker, M., 2013. Irrigation, soil organic carbon and N2O emissions. A review. Agron. Sustain. Dev. 33 (4), 733–749. https://doi.org/10.1007/s13593-013-0134-0.
Walthert, L., Graf, U., Kammer, A., Luster, J., Pezzotta, D., Zimmermann, S., Hagedorn, F., 2010. Determination of organic and inorganic carbon, delta C-13, and nitrogen in soils containing carbonates after acid fumigation with HCl. J. Plant Nutr. Soil Sci. 173 (2), 207–216. https://doi.org/10.1002/jpln.200900158.
Wei, T., Simko, V., Levy, M., Xie, Y., Jin, Y., & Zemla, J. (2013). corrplot: Visualization of a correlation matrix. *R package version 0.73*(230), 11.
Whitaker, J., Ostle, N., Nottingham, A.T., Ccahuana, A., Salinas, N., Bardgett, R.D., McNamara, N.P., 2014. Microbial community composition explains soil respiration responses to changing carbon inputs along an Andes-to-Amazon elevation gradient. J. Ecol. 102 (4), 1058–1071. https://doi.org/10.1111/1365-2745.12247.
Wilson, H.F., Xenopoulos, M.A., 2009. Effects of agricultural land use on the composition of fluvial dissolved organic matter. Nat. Geosci. 2 (1), 37–41. https://doi.org/10.1038/Ngeo391.
Wolf, K., Flessa, H., Veldkamp, E., 2012. Atmospheric methane uptake by tropical montane forest soils and the contribution of organic layers. Biogeochemistry 111 (1–3), 469–483. https://doi.org/10.1007/s10533-011-9681-0.
Zhang, Y., Li, J.T., Xu, X., Chen, H.Y., Zhu, T., Xu, J.J., Nie, M., 2023. Temperature fluctuation promotes the thermal adaptation of soil microbial respiration. Nat. Ecol. Evol. https://doi.org/10.1038/s41559-022-01944-3.
Zsolnay, A., 1996. DISSOLVED Humus in Soil Waters. Elsevier Science BV.
Zsolnay, A., Baigar, E., Jimenez, M., Steinweg, B., Saccomandi, F., 1999. Differentiating with fluorescence spectroscopy the sources of dissolved organic matter in soils subjected to drying. Chemosphere 38 (1), 45–50. https://doi.org/10.1016/S0045-6535(98)00166-0.